ADDIS ABABA UNIVERSITY
ADDIS ABABA INSTITUTE OF TECHNOLOGY
SCHOOL OF CIVIL AND ENVIRONMENTAL ENGINEERING

Experimental Investigation of the Role of Coarse Aggregate for Bond Strength of Reinforced Concrete

---

A Thesis in Structural Engineering

By Lemlem Abebaw
May 7, 2021
Addis Ababa

A Thesis
Submitted in Partial Fulfillment of the Requirements for the Degree of Master of Science

The undersigned have examined the thesis entitled '**Experimental Investigation of the Role of Coarse Aggregate for Bond Strength of Reinforced Concrete**' presented by Lemlem Abebaw, a candidate for the degree of Master of Science, and hereby certify that it is worthy of acceptance.

Dr. Esayas Gebreyouhannes	______________________	_________________
Advisor	Signature	Date
Dr.-Ing. Adil Zekaria	______________________	_________________
Internal Examiner	Signature	Date
Prof. Girma Zerayohannes	______________________	_________________
External Examiner	Signature	Date
Dr.-Ing. Mebruk Mohammed	______________________	_________________
School Dean	Signature	Date

UNDERTAKING

I, the undersigned, certify that the research work titled "**Experimental Investigation of the Role of Coarse Aggregate for Bond Strength of Reinforced Concrete**" is my work. The work has not been presented elsewhere for assessment. Where material used from other sources has been properly referred.

Lemlem Abebaw

Signature____________

Date May 7, 2021.

DEDICATION

Dedicated to Eshetie, it's always my greatest motivation to make you proud.

ABSTRACT

Beam-column joints have a critical role in the integrity of structures. Due to reinforcement bars are anchored and lap into the column, joints are one of the most congested structural components. Placing and consolidating concrete in such structural frames imposes substantial technical challenges, which restricts the flow of coarse aggregates, thereby creating voids. Bond is the only way that transfers the tensile stresses between concrete and reinforcements. It is influenced by numerous factors such as the diameter of bars, concrete strength, embedded length of bars, concrete cover, reinforcement yield strength. In this research, another factor which is coarse aggregate size is considered, the role of coarse aggregate for bond strength of reinforced concrete was investigated experimentally using cylindrical samples (300*150mm) with centrally embedded 14 mm and 16mm deformed bar. A total of thirty-nine pull-out tests were carried out to determine the bond. Six mixes of concrete with similar compressive strengths but different coarse aggregate sizes of 37.5mm, 25mm, 19mm, 12.5mm, 9.5mm, and pure mortar were used with bar sizes of 14mm and 16mm. Compressive strengths of all concrete kept at the same level to study only the effect of coarse aggregate size on bond strength. Compressive strength, splitting tensile strength, and bond strength for normal strength concrete were studied. The bar was subjected to a monotonic axial load at the loaded end while the other end was embedded in concrete. Test results show the bond strength decreases significantly with a decrease in coarse aggregate size, there is a drop in bond strength especially at the pure mortar, despite having the same compressive and splitting tensile strengths. The research work outcome indicates, bond strength is highly affected by the coarse aggregate size, it has a significant difference between concrete contain the larger coarse aggregate size and pure mortar, which is about 38.65% and all specimen’s failure mode was by pullout for those who have $5d_b$ embedment length. The bond strength for different coarse aggregate sizes was compared to equations proposed by different researchers and current codes. CEB-FIB 2010 codes, Esfahani & Rangan, Orangun et al and Darwin et al bond strength calculation equation works well only when the coarse aggregate size is 25mm and 19mm. Therefore, aggregate size is critical for bond strength when smaller coarse aggregates sizes are used.

Keywords: Beam-Column Joint, Coarse Aggregate size, Bond Strength, Pull out Test

ACKNOWLEDGMENTS

Above all, I would like to praise the almighty God for giving me the strength, perseverance, and provision to accomplish this thesis.

I would like to express my deepest gratitude and respect to my advisor Esayas G.Youhannes (PhD.), for his incredible support, inspiration, supervision, and constructive comments throughout the thesis. I am inspired by his dedication and research abilities.

I also extend my acknowledgment to give immense credit to Ing. Eshetie Tesfaye. This accomplishment would not have been possible without his imperative help. He has also been there in every step throughout my years of study and during this research; there is no doubt that a single step further is unthinkable without his involvement. I have nothing to say except to remain in debt i cannot be able to repay even if i serve him till my last day on earth.

I would like to sincerely thank Abraham Asefa(PhD.), and Euyel for letting me use the pull-out machine for the experiment.

I would also like to acknowledge the school of graduate studies of AAU for the waived tuition and research fee scholarship granted.

Furthermore, I would like to forward my esteemed appreciation to Jemal Kedir and Kalkidan Tesfaye, who made the laboratory work simpler with their valuable assistance.

Last but foremost, I would like to expand my gratitude to all those who have directly and indirectly helped me throughout my research.

TABLE OF CONTENTS

LIST OF TABLES

LIST OF FIGURES

LIST OF ABBREVIATIONS

BCJ	Beam-Column Joint
CA	Coarse Aggregate
EBCS	Ethiopian Building Code Standard
NSC	Normal Strength Concrete
OPC	Ordinary Portland Cement
RC	Reinforced Concrete

NOTATION

C	Cover depth
d_b	Bar diameter
l_b	Embedment length

1. INTRODUCTION

1.1. Background

Beam-column joints have a critical role in the integrity of structures. The structural design and analysis of frames are usually following the assumption that the beam-column joints perform as rigid bodies. The presumption that the joint is rigid fails to take the effects produced within the joint into account. Due to reinforcement bars are anchored and lap into the column, joints are one of the most congested structural components. Placing and consolidating concrete in such structural frames imposes substantial technical challenges, which restricts the flow of coarse aggregates, thereby creating voids. Concrete is a combined material whose behavior depends on its constituent materials' behavior. Cement, aggregates, and water are the main components of concrete. Depending on the mix proportion of concrete 60-75% by volume and 70 to 85 % by weight is an aggregate aggregates are commonly assumed as an inert filler in concrete. However, a closer look indicates the aggregate influence properties of both hardened and fresh concrete. Changes in maximum size, moisture content, gradation, and unit weight of coarse aggregate can all vary the performance and character of the concrete[1].

Bond strength is characterized as the measure of the effectiveness of the grasp between concrete and steel. This factor is very crucial to develop the composite behavior of reinforced concrete which is comprised of two components with different mechanical behavior and physical features. In general, when the load is applied to the reinforced structure the steel-to-concrete bond allows longitudinal forces to be transferred between reinforcement and the surrounding concrete. It is well known that the overall behavior of rc structures is highly dependent on the interaction between steel and concrete. Therefore, to ensure the safety of concrete, proper bonding between reinforcing steel and concrete is essential. If the resistance of the bond is inadequate, reinforcement bar slippage occurs, breaking the composite action. Brittle failure will occur due to sudden loss of bond between rebar’s and concrete in anchorage zones in rc members[2].

The efficiency of the rc joint is subject to numerous factors, joint reinforcement, eccentricity, concrete grade, column axial load, and bond strength. Therefore, it's important to discuss critical parameters that affect joint performance with special regard to bond strength. Many of the experimental tests on concrete structures have relieved that, the bond stress between reinforcement and concrete is going to be reduced at the joint, prominent to the

loss of joint capacity and stiffness, and finally the bond and anchor failure of the steel bar at the joint position typically caused the structural failure of the frame. Understanding the joint behavior is important in working out proper outcomes within the design of beam-column joints. Bond strength is influenced by numerous factors like the diameter of bars, concrete strength, embedded length of bars, concrete cover, reinforcement yield strength[3].

The bond strength between concrete and reinforcing steel bars has been extensively studied. Nevertheless, comparatively, attention isn't given to see the role of coarse aggregate for bond strength of rc structure. The steel-concrete bond allows the tensile forces to be transferred between the concrete and the steel. Bond strength is principally littered with reinforcement properties like the surface profile and sort of steel rebar instead of those associated with aggregate properties[4]. However, another researcher revealed that the bond strength might increase with the increasing coarse aggregate amount in concrete[5]. A lot of effort within the past has been dedicated to the improvement of the bond characteristics within the interface zone between bar and concrete from a reinforcement point of view. Less has been done on the enhancement of bond strength from a concrete point of view. Therefore, the main aim of this research is to study the role of coarse aggregate for bond strengths of concrete. Experimentally, these aspects were addressed by conducting a pull-out test considering as parameters coarse aggregate size, and embedment length.

1.2. Statement of the Problem

The performance of beam-column joints and the key factors that affect them aren't yet entirely understood and widespread for all structural engineers. placing and consolidating concrete is incredibly troublesome within the Beam-column Joint as a result of the congested reinforcement bar arrangement. Structural engineers design Beam-column Joint as there's coarse aggregate at the zone since there's an extremely congested bar arrangement at the Beam-column Joint coarse aggregate won't pass into the zone. The poor design practice of beam-column joints endangers the whole structure, even though the rest structural members adapt to the design necessities [6]. In this research, an experimental investigation was carried out to study the role of coarse aggregate size for bond strengths of concrete, where aggregate covers a prominent contribution.

1.3. Objectives of the Study

1.3.1. General Objective

The general objective of this study was to investigate the role of coarse aggregate for bond strengths of reinforced concrete.

1.3.2. Specific Objective

The specific objective of this study:

- ✓ To compare equations proposed by different researchers and current codes for the different coarse aggregate sizes of bond strength.

1.4. Scope of the Study

In this research, the role of coarse aggregate for bond strength of reinforced concrete using pullout test subjected to monotonic load was investigated. In this study only Normal Strength Concrete (NSC) Concrete grade was used.

1.5. Significance of the Study

Usually, the design of reinforced concrete structural elements is concentrated on the design of beams and columns and, sometimes, it's not given equivalent attention to the beam-column joints. The results of this research attempt to contribute to the efforts of structural engineers to consider the role of coarse aggregate for reinforced concrete while they are designing congested structural elements. Since design codes are not considered the effect of coarse aggregate size in the proposed equation this research has tried to clearly show the contribution of coarse aggregate for bond strength. So it suggests the code takes into account the coarse aggregate size effect in the proposed equation to attain the required bond strength and to prevent bond failure at beam-column joints.

1.6. Organization of the Thesis

The thesis comprises five chapters and organized as follows.

Chapter one provides a general introduction to the thesis with a brief content of the background information and explores the rationale of the research by highlighting the main issues associated with Coarse Aggregate and Bond Strength, objectives, and scope as well as the organization of the thesis. Chapter two reviews the relevant literature, and quotes the various related works done in the study area. Chapter three presents the materials, methods, and testing procedures. Chapter four attempts to describe in detail the results of the experiments, followed by discussions of the findings. Finally, Chapter five includes conclusions and recommendations of the study.

2. LITERATURE REVIEW

2.1. Introduction

In this chapter, the review of relevant literature on bond strength, bond-slip, beam-column joint behavior, and testing techniques of the specimen to evaluate the bond strength of reinforced concrete are discussed.

2.2. Bond

Bond is the key factor in facilitating an RC structure to work as a single element by allowing the transfer of stress between the reinforcing bar and the surrounding concrete. Bond is a measure of interaction between concrete and the bar, measured by bond stress. It is an important parameter and significantly affects joint behavior. For reinforced concrete to perform as intended, a bond must be established on the interface between steel and concrete, to avoid significant slip from occurring at that boundary.

2.3. Bond-Slip-Strain Relationship

The bond-slip association expresses the local bond stress at any location along a bar as a function of the local slip[7].

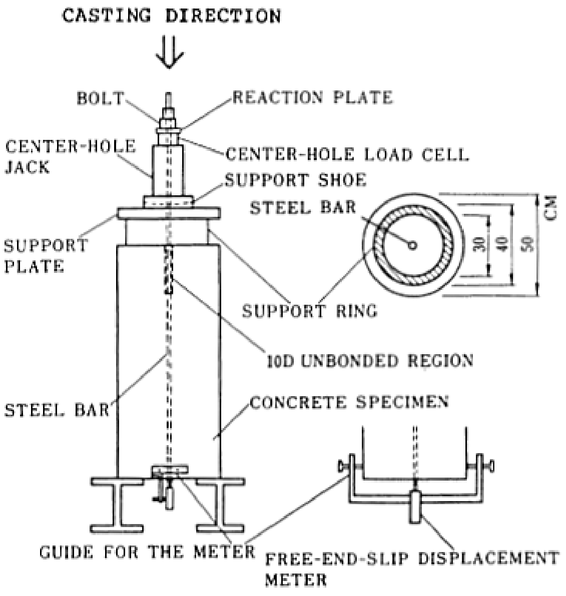

Figure 2.1. Pullout test setup

The internal local slip at any point is defined by

$$s = \int_{xo}^{x} \varepsilon dx + s_o \qquad (2.1)$$

In pullout tests, a slip is obtained by taking the summation of the free end slip S_o and the integration of strains from the free end (x_o) to the point concerned (x).

The local stress at the associate location on an embedded bar is so proportional to the slop of the strain distribution curve at that point. At any point, the bond stress τ is expressed as

$$\tau = \frac{ED}{4}\frac{d\varepsilon}{dx} \qquad (2.2)$$

Where

E is the young's modulus of the bar,

D is the bar diameter and

$\frac{d\varepsilon}{dx}$ is the slope of the strain distribution curve.

The Bond-slip relationship for both pull-out and splitting failure is shown in Figure 2.2 [8]

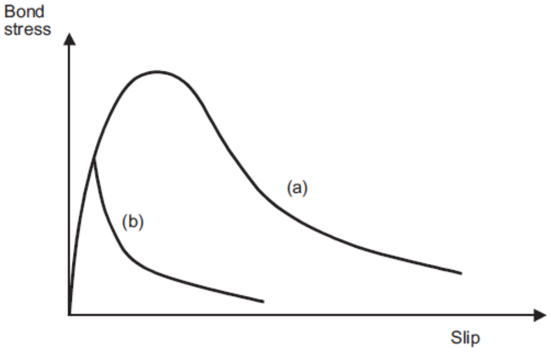

Figure 2.2. Schematic bond-slip relationship: (a) pull-out failure; (b) splitting failure

COMMON BOND TESTS

There are four common bond test arrangements, beam-end specimens, splice specimens (full beams), pull-out specimens, and beam anchorage specimens. The direct pull-out test way is one the most usually used because of the simplicity of testing and fabricating of the specimens.

Definition of tensile stress and bond stress

A common supposition for the RC structural design is that the reinforcement bar is loaded in a longitudinal direction only. In bond strength tests, the boundary conditions are expressed by the unstressed unloaded end and the stressed loaded end as shown clearly in Figure 2.3[9].

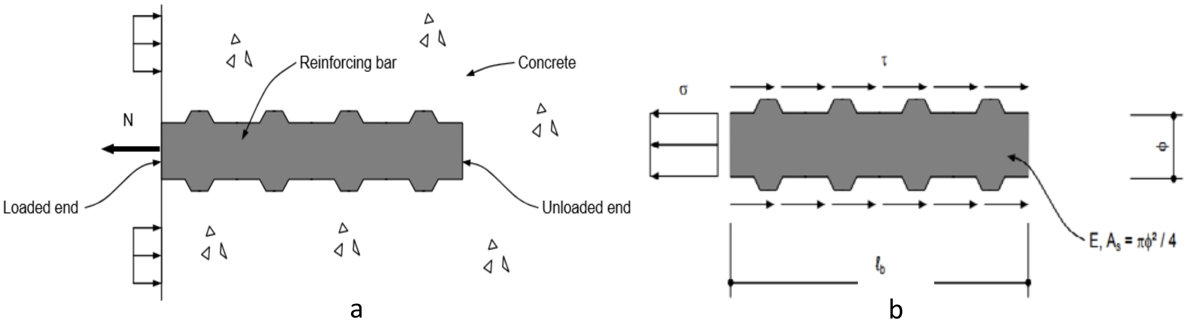

Figure 2.3 Schematic of pullout test (a); tensile stress and bond stress of a reinforcing bar element with one loaded and one unloaded end (b)

Bond stress-slip model

In an RC structure, when the strain in the concrete (ε_c) is not the same as the strain in the bar (ε_s), slip occurs and bond transfer must follow through the embedment length, to withstand the applied loading. The average bond stress (μ_{avg}) was derivative from the anchorage bond stress based on BS 8110[10].

$$\mu_{avg} = \frac{Fs}{\pi * \phi * l} = \frac{f_s * \phi}{4 * l} \tag{2.3}$$

Where

Ø is the bar diameter,

F_s is the bar force

f_s is the steel stress, and

l is the embedment length.

Bar stress distribution during a pull-out test is shown clearly in Figure 2.4[11].

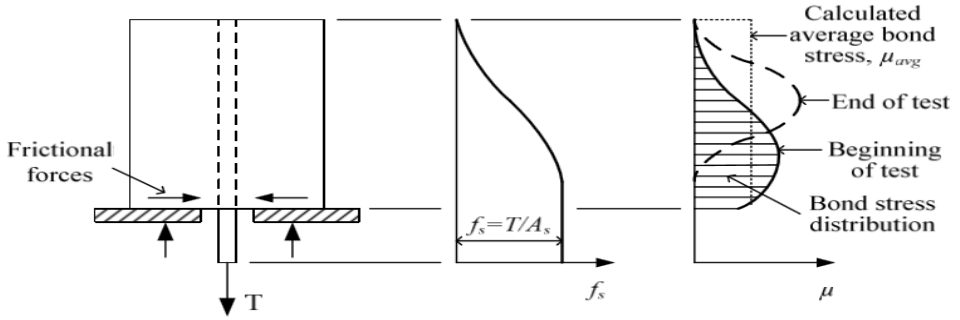

(a) Test Method (b) Bar Stress (c) Bond stress

Figure 2.4. Theoretical distribution of bar stress during a pull-out test[11]

It is challenging to assess the distribution of bond stress along the length of the bar embedded in the concrete because the force carried by the steel bar varies from the free-end to the loaded-end due to load transfer. Therefore, the local strain of the steel bar within the concrete is equivalent to the average strain of the surrounding concrete[12].

Constitutive law of bond

The constitutional law of bond is also termed as a bond stress-slip relationship. Representative bond stress-slip curves of monotonic bond tests on reinforcing bars with a short embedment length shown in Figure 2.5[13].

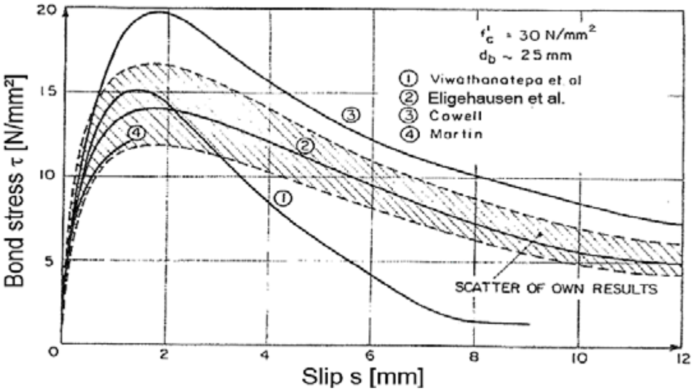

Figure 2.5. Bond stress-slip curves[13]

The bond stress-slip association be determined by numerous aspects, such as; concrete strength, bar type (plain and deformed), the boundary conditions, bar roughness, concrete cover, and bar position at the time of casting. Bond stress versus slip for ribbed bars in the elastic range is shown in Figure 2.6[14].

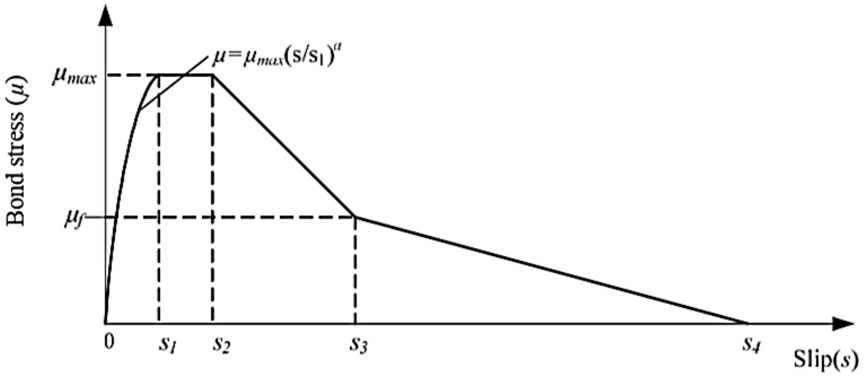

Figure 2.6. Bond stress versus slip in the elastic range[14]

The simplest way to measure the bond stress-slip association is the direct pull-out test which has been used comprehensively to evaluate the level of bond that develops between a steel bar and concrete [11]. Bond stress is shear stress at the concrete-bar interface which, by transmitting loads between the surrounding concrete and the bar. This bond, when well developed, allows the two materials to form a composite structure[15], [16].

2.4. Mechanics of Bond Slip

The bond strength between rebar and concrete is made up of three main mechanisms: mechanical bearing between the ribs of deformed bars and surrounding concrete, friction due to the roughness of the interface, and chemical adhesion between steel and concrete[3].

The bond strength of plain bars depends mainly on the Friction, and Chemical adhesion while on deformed bars, the bond resistance capacity is primarily governed by the mechanical bearing accomplishment. Adhesion is the stick-like bond between the steel and the concrete on the un-deformed part of the reinforcing bar. Bearing resistance is the pushing force of the concrete counter to the deformation of the steel bar. Friction is the resistance of effort caused by the concrete-steel association on the deformed part of the bar. The three main mechanisms of bond-slip between rebar and concrete are shown in Figure 2.7[11], [17].

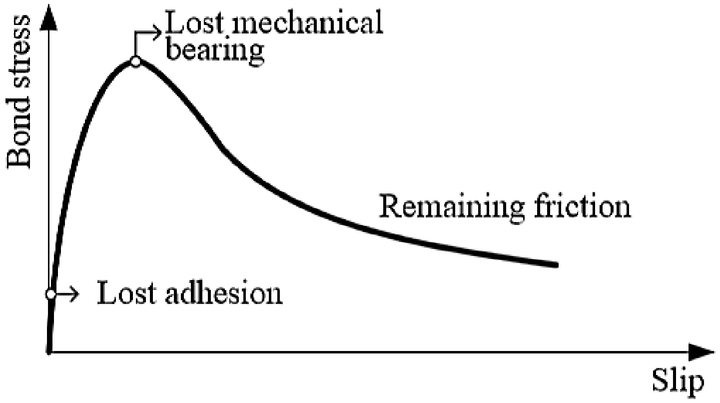

Figure 2.7. Simplified bond stress-slip behavior[17]

In the tension zone, the transfer of tension force from the reinforcement to the nearby concrete is by shear at the concrete-bar interface. This interface shear is called bond stress. The system by which the bars develop this bond is by adhesion (bar surface and concrete) and by friction in the first loading. As loading carries on both the adhesion and friction influence would be lost and the bond will be transmitted by the bearing on the deformation of the bars.

2.5. Beam-Column Joint Behavior

The joint is the part of the column within the depth of the beam that connects into the column. Failure of joints is governed by shear and bond failure mechanisms which are brittle. Joints with a high reinforcement ratio require, not only a higher volume of concrete in compression, as well as concrete with high strength, to take advantage of all capacity of the tensioned rebar[6].

Joint is that the critical zone in an RC moment-resisting frame. The issues of detailing and construction of joints are often not valued by designers. Indeed, the contradictory necessity of a small size bar for good performance and large size bars for ease of concreting and placement is more noticeable at the joints than anywhere else. The design of interior joints in a reinforced concrete frame structure points to a problem of proper force transmission through the joints since large shear forces develop in beam-column joints [18] Bars, that go through the interior joints, are exposed to ‘pushing’ and ‘pulling’ of the nearby beams to transfer the force from steel to the surrounding concrete.

Shear force is transmitted in the interface zone between concrete and steel by bond stresses, which can be extremely large and exceed material bond strength. Bond stresses that exceed the bond strength, established at the concrete-bar boundary, might cause in bond-slip. loss in bond strength may cause a loss of about double the amount of the energy dissipation capacity in a typical joint [19].

Pauley[18] considered the bond behavior between the bar and concrete for the interior joint core. Bond slip is the system that refers to the movement of the longitudinal bar from the surrounding concrete due to a drop of the bond strength between the two.

Pauley et al. [18] suggested that the bond in a joint is typically affected by the yield penetration of bars into the joint from the nearby plastic hinges, which ultimately causes bar pullout or the separation between nearby beam, column members, and joint element. Pauley et al. also put forward that a uniform bond stress distribution along the elastic portion of the longitudinal reinforcement is a probable solution to quantify the bond behavior.

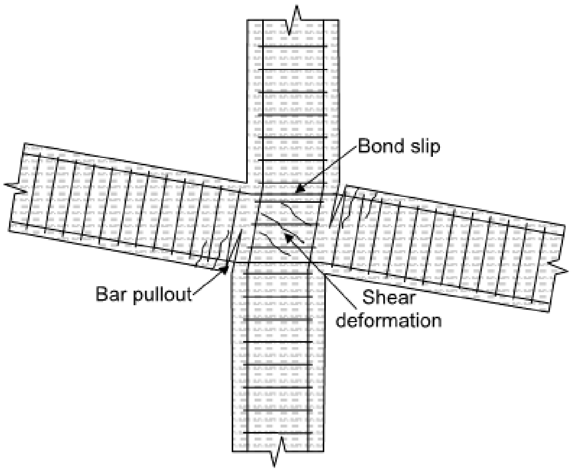

Figure 2.8. Joint with bar pullout and bond-slip

Relative displacement between steel bars and surrounding concrete is recognized to be very large at connections of members. A large crack occurs at the connection due to the pullout of the anchored bar.

2.6. Strain Gauge Installation

To overcome possible damage to strain measuring systems during both the manufacture and testing of a specimen's different approach has been adopted.

Two main problems make it difficult to accurately measure the local bond-slip association. The primary is that the steel bar is embedded within the concrete making it difficult to monitor the local changes of strain over a given length. The second issue is that reinforcement bar yielding, which can happen before deboning, will considerably affect the bond-slip performance.

Surface Mounted

In this approach, strain gauges are attached straight on top of the surface of the steel bar to measure the strain. During the fabrication of the specimen as the aggregate can damage the gauge or the electrical wires, it leads to high failure before testing. Also due to the relative movement that can occur at the steel/concrete interface, this can give rise to damage to the strain gauge or the connection between the gauge and any associated wires[20], [21].

Central Groove Mounted

A longitudinal groove running down the middle of the reinforcing bar, this method is more time consuming, and expensive, than the use of simple surface-mounted gauges but produces an instrumented bar with the external appearance of a conventional reinforcing bar. Besides there remain concerns regarding the continuity of the material properties of the instrumented bar which may impact the bond stress behavior due to the ways that the two halves of the split bar are held together, using either tack welds mains 1951 [22] or epoxy resin glue Scott and gill 1987[23].

Near Surface Mounted

To some degree simpler method than the central-groove method was find out by Weathersby [24]who attached the wires, and strain gauges inside two grooves, machined along the longitudinal rib on both sides of the reinforcing bar. A parallel method was adopted by Lee and Mulheron[17] who use a single surface groove to attach the strain gauges and provide a place to stay the connected wires. Using records from this approach it has been revealed that in the post-peak region the bond stress increases linearly from the free end of the bar.

2.7. Bond Strength Equations in Code Provisions and Empirical Equations

Bond behavior can be determined using various types of bond tests, including standardized tests with a short bond length such as the RILEM pull-out test [25], or a procedure by ASTM [26]. The bond length with small pull-out samples in experiments is usually limited to five times the bar diameter, which is assumed to represent the behavior of an incremental bond element.

In fib MC2010 [27]a minimum cover depth equaling the diameter of the embedded bar is suggested, to avoid premature bond failure and therefore lower bond stress due to splitting of the concrete cover.

Equations in code provisions

Different codes have put forward equations for estimating the bond strength between surrounding concrete and steel reinforcement taking into consideration the main parameters such as bar diameter, compressive strength, concrete cover, and embedment length.

The American Concrete Institute (ACI) 318 [28] **and the Canadian Standards Association (CSA) CAN3-A23.3**[29] **codes** provide equations that account for the developmental length of deformed rebar. The minimum required bond strength can then be calculated based on the calculated development length as:

$$\tau = \frac{f_y A_b}{\pi d_b l_d} \tag{2.4}$$

where

f_y is the yield strength of rebar, and

A_b is the area of rebar

d_b is the bar diameter

l_d is the development length

According to the ACI code provision [28] the development length (l_d) of No. 19 and smaller deformed bars in tension can be calculated as:

$$l_d = \left(\frac{f_y \psi_t \psi_e \ \psi_s \lambda}{2.1\sqrt{f_c'}} \right) d_b \tag{2.5}$$

Where

f_y is the yield strength of rebar, and

ψ_t is the location factor

ψ_e is the coating factor

ψ_s is the reinforcement size factor

λ is the type of concrete

$f_c{}'$ is the concrete's compressive strength

d_b is the bar diameter

The CSA code has the same equation as the ACI to estimate the development length of reinforcement rebar. The key variation between the ACI and CSA codes is the rebar diameter factor. According to the ACI, the rebar diameter factor is decreased from 1.0 to 0.8 if the bar diameter is equal to or less than 6 mm (For No. 6, smaller bars and deformed wires, reinforcement size factor(ψ_s) = 0.8. For No. 7 and larger bars, ψ_s = 1.0); in the CSA code, the rebar diameter factor is decreased from 1.0 to 0.8 if the rebar is equal to or less than 20 mm diameter.

Australian Standard 3600 [30] put forward the following equation:

$$\tau_u = 0.265\sqrt{f_c'\left(\frac{c}{d_b} + 0.5\right)} \tag{2.6}$$

where

$f_c{}'$ is the concrete's compressive strength

c is the radius of a cylinder concrete specimen

d_b is the bar diameter

In the **CEB-FIP model code** [31] for the bond strengths, between the surrounding concrete and the deformed bars under monotonic loading is defined as shown.

$$\tau_u = 2.5\sqrt{f_c'} \quad \text{at pull-out failure} \tag{2.7}$$

JSCE code- concrete design bond strength proposed by the **JSCE code**[32] as

$$\tau = 0.28 f_c'^{\frac{2}{3}} (\tau \leq 3.7\text{MPa}) \quad (2.8)$$

where

f_c' is the concrete's compressive strength

Ethiopian building code

The bond strength according to ESEN 1992 1-1:2015[33]is given by the following Equation

$$f_{bd} = 2.25 \eta_1 \eta_2 f_{ctd} \quad (2.9)$$

Where

f_{ctd} concrete tensile strength, $f_{ctd} = \frac{\alpha_{ct} f_{ctk0.05}}{\gamma}$

η_1 A coefficient associated with the position of the bar during concreting and, the quality of the bond condition

η_2 Related to the bar diameter

The bond strength, defined as the average bond stress along the bar length, is calculated by dividing the bond failure load by the bonded surface area of the steel bar as given below.

$$f_{bd} = \frac{T}{\pi d_b l_b} \quad (2.10)$$

To calculate the tensile force needed to pull out the steel reinforcement bar embedded in concrete

$$T = f_{bd} A \quad (2.11)$$

Where

T is the tensile force used to pull out a reinforcement bar embedded in concrete

d_b (mm) is the diameter of the test bar

l_b (mm) is the embedment length (concrete depth-concrete cover)

Empirical equations

Equations that represent the bond strength between the concrete and the steel bars have been suggested by several researchers, as follows.

Orangun et al.[34] Proposed the following formula:

$$\tau_u = 0.083045\sqrt{f_c^{'}}\left(1.2 + 3\frac{c}{d_b} + 50\frac{d_b}{l_d}\right) \tag{2.12}$$

Where

c is the minimum concrete cover and

$f_c{}'$ is the concrete's compressive strength

d_b is the diameter of the bar

l_b is the embedment length

Darwin et al.[35] Proposed a modified expression for the bond strength as:

$$\tau_u = 0.083045\sqrt{f_c^{'}}\left(2.12\left(\frac{c}{d_b} + 0.5\right)\left(0.92 + 0.08\frac{c_{max}}{c_{min}}\right) + 75\frac{d_b}{l_d}\right) \tag{2.13}$$

Where C_{min} = min (C_x, C_y, C_s/2), C_{max} = max [min (C_x, C_s/2), C_y],

C_s is the spacing between the bars,

C_x is the side cover, and

C_y is the bottom cover.

Esfahani & Rangan [36]

$$\tau_u = 8.6\frac{\frac{c}{d} + 0.5}{\frac{c}{d} + 5.5} f_{ct} \tag{2.14}$$

Where *fct* is the tensile strength of concrete taken as 0.55 *fc*.

In 1987, **Shima** [7] reported the following bond models that can predict the tension stiffening effect and that can be used under any boundary condition. Propose the following Equation for the bar with a short and a long embedment, respectively, while taking to account the strain effect following the boundary conditions.

$$\tau = 0.73 f_c'^{\frac{2}{3}} \left[\ln\left(1 + 5000\frac{s}{d_b}\right)\right]^3 * \frac{1}{1 + 10^5 * \varepsilon_s} \tag{2.15}$$

$$\tau = 0.9 f_c'^{\frac{2}{3}} \left[1 - e^{-40\left(\frac{s}{d_b}\right)^{0.6}} \right] \tag{2.16}$$

Where

f_c' is the compressive concrete strength,

s is the slip

d_b is the bar diameter,

ε_s is the strain of the bar.

3. MATERIAL AND METHODS

3.1. Introduction

In this chapter, properties, and types of materials, all laboratory tests, sample preparations, experimental procedures, and test setups used in the study are briefly described. The materials are prepared, tested and details of the experimental program were conducted in the construction material laboratory of Addis Ababa Institute of Technology (AAiT). The properties of each material and testing are checked whether they comply with the requirements set in ASTM standards and specifications.

3.2. Materials

The material used for this research includes cement, fine aggregate, coarse aggregate, water, and reinforcement bar.

3.2.1. Cement

Commercially available Ordinary Portland Cement from the local market was used during this study. The cement used in this study is Type-1 Dangote an ordinary Portland with CEM 42.5 R grade and the physical properties of the cement were examined, the relative density of 3.15g/cm^3.

3.2.2. Aggregate

Aggregate is a broad term, which includes a coarse and fine aggregate. Minimum three-quarters of concrete are covered by aggregate. In this research, the aggregate was supplied from the same source to eliminate any variations due to a different source. All relevant laboratory tests such as bulk density, specific gravity, and moisture content of the aggregate have been tested to ensure that the material meets the specification for concrete work. Before the determination of aggregate properties, it was washed to remove impurities like silt, organic material, and any other dust which reduces its quality. Besides that, the aggregate was kept in a plastic bag after it dried until the time of mixing to maintain the moisture content.

3.2.2.1. Fine Aggregate

Fine aggregates used in concrete are small-size filler material that passes through a 4.75mm sieve and retains on sieve 0.07mm sieve [37]. For this study, the fine aggregate was collected from the Werabe River passing through a 4.75mm sieve. The physical properties of fine aggregate got from laboratory test results are summarized in Table 3.1 below.

Table 3.1. Physical properties of Fine aggregate

No.	Test description		Test result
1.	Silt content		0.37%
2.	Moisture content		1.71%
3.	Absorption capacity		3.63%
4.	Finesse modulus		2.63%
5.	Unit weight		1516.3Kg/m^3
6.	Specific gravity	Bulk	2.44 g/cm^3
		The bulk (SSD)	2.53 g/cm^3
		Apparent	2.67g/cm^3

Table 3.2. The particle size distribution of fine aggregate

Sieve Size(mm)	Weight Retained (g.)	Percent Retained (%)	Cumulative Retained (%)	Cumulative Passing (%)	ASTM C 33 Standard passing range (%)
4.75	0	0	0	100	95-100
2.36	32	5	5	95	80-100
1.18	71	16	21	79	55-85
0.6	128	27	48	52	25-60
0.3	214	43	91	9	5-30
0.15	47	7	98	2	0-10
Pan	8	2	100	0	0

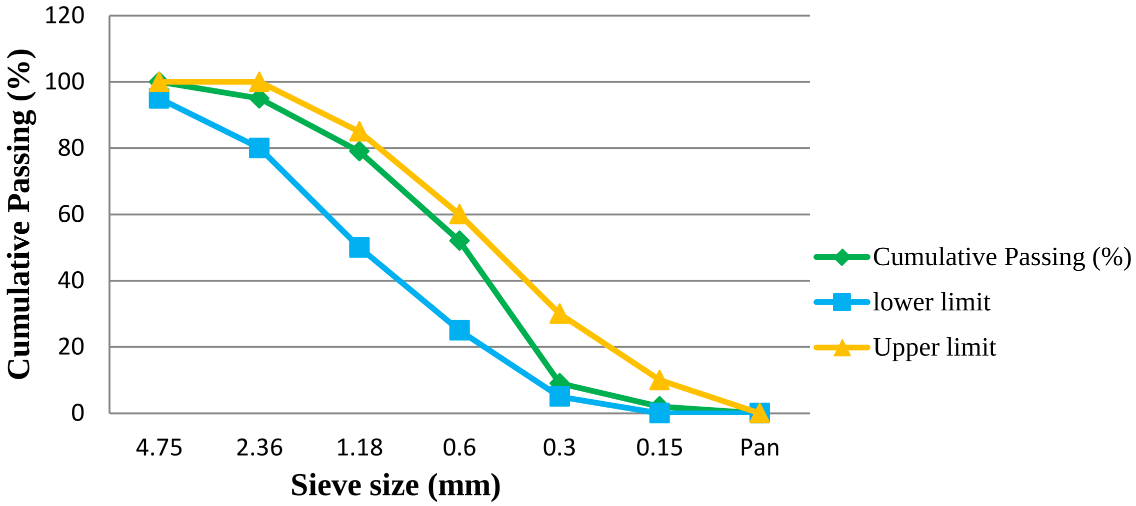

Figure 3.1. Gradation curve of fine aggregate

The fine aggregate was washed to minimize its silt content from 7.4% (original silt content) to 0.37%. The local fine aggregate used for this study satisfies ASTM C-33-01[38] requirement.

Figure 3.2. Silt content of fine aggregate

3.2.2.2.Coarse Aggregates

The aggregate used for this research is basaltic crushed rock coarse aggregates, supplied by a local material supplier. Five different coarse aggregates having different coarse aggregate sizes i.e. 9.5mm, 12.5mm, 19mm, 25mm, and 37.5mm were used. The physical properties of coarse aggregate obtained from laboratory test results as per ASTM are summarized in Table 3.3 and Figure 3.8 below.

Table 3.3. Physical properties of the Coarse Aggregate

No.	**Test Description**		**Results**
1.	Moisture Content		1.52%
2.	Unit weight		1569.16kg/m³
3.	Fineness modulus		3.65
4.	Absorption capacity		1.96%
5.	Specific gravity	Bulk	2.81g/cm^3
		The bulk (SSD)	2.87g/cm^3
		Apparent	2.98g/cm^3

Table 3.4. The particle size distribution of the Coarse Aggregate

Sieve Size(mm)	**Weight Retained (kg)**	**Percent Retained (%)**	**Cumulative Retained (%)**	**Cumulative Passing (%)**	**ASTM C 33 Standard passing range (%)**
37.5	0	0	0	100	100
25	5.15	35.36	35.36	64.64	90-100
19	3.89	23.2	58.56	41.44	40-85
12.5	3.01	22.8	81.36	18.64	10-40
9.5	1.73	9.23	90.59	9.41	0-15
4.75	1.13	8.67	99.26	0.74	0-5
pan	0.09	0.74	100	0	0

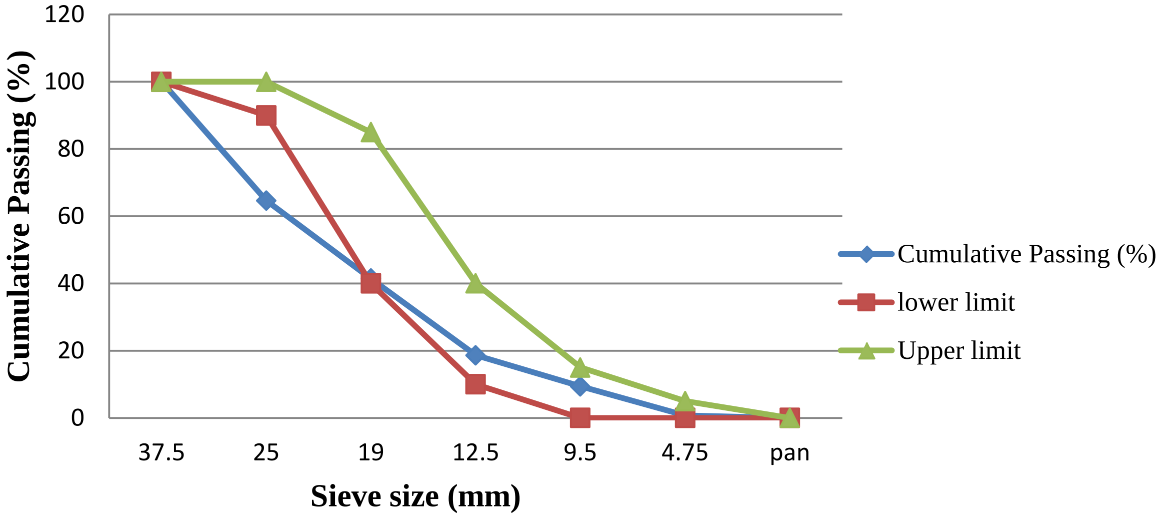

Figure 3.3. Gradation curve of Coarse aggregate

3.2.3. Water

Water is an essential component of concrete as it strongly plays a part in the chemical reaction with cement. Moreover, to mix the concrete, the curing of concrete and washing of aggregate has been done by water. Therefore, water must not contain impurities such as alkalis, suspended solids, acids, silt, clay, and dissolved salt that cause degradation in quality. Accordingly, the water used for this research is tap water from the construction material laboratory of Addis Abeba institute of Technology water supply pipe.

3.2.4. Reinforcement Bar

In all test specimens, normal strength deformed reinforcements available in the local market (Turkey imported/ produced) were used. A uniaxial tension test was conducted on sample reinforcements to determine the mechanical properties as shown in Figure 3.4. The mechanical properties of the reinforcements are given in Table 3.5.

Table 3.5. Mechanical properties of reinforcements Bars

Diameter	**Average Diameter (mm)**	**Modulus of elasticity (GPa)**	**Average Yield load (kN)**	**Average Failure load (kN)**	**Average Yield strength (MPa)**	**Average Ultimate strength (MPa)**
Φ14	14.06	200*	85.33	104.33	549.61	671.97
Φ16	16.29	200*	131.90	148.27	632.61	711.13

* *Assumed value*

Figure 3.4. Tensile strength testing machine

3.3. Specimens

The Specimens are selected based on coarse aggregate size. The coarse aggregate in Specimens CA37.5 (37.5mm), CA25 (25mm), CA19 (19mm), CA12.5 (12.5mm), and CA9.5 (9.5mm) is normal weight aggregate.

Table 3.6. Test types and number of specimens

Coarse Aggregate size (mm)	**E.L (mm)**	**U.L.L and U.L.F (mm)**	**Pull out Test**	**Compressive test**		**Splitting Tensile Test**	
			28 day	**7 day**	**28 day**	**7 day**	**28 day**
37.5	70	115	3	3	3	3	3
25	70	115	3	3	3	3	3
19	70	115	3	3	3	3	3
12.5	70	115	3	3	3	3	3
9.5	70	115	3	3	3	3	3
Pure mortar 1	70	115	3	3	3	3	3
25	150	75	3	_	_	_	_
19	150	75	3	_	_	_	_
12.5	150	75	3	_	_	_	_
9.5	150	75	3	_	_	_	_
Pure mortar 2	150	75	3	_	_	_	_
Pure mortar 3	200	50	3	_	_	_	_
Pure mortar 4	250	25	3	_	_	_	_
Total number of specimens			**39**	**36**		**36**	

Embedment length (E.L), unbonded length at the loaded end (U.L.L), and Unbonded length at the free end (U.L.F)

Fresh and hardened concrete properties were investigated for each mix. Workability was investigated on the fresh concrete while compressive strength, splitting tensile strength, and bond strength was studied on the hardened concrete. Hence, a total of 30 cubes of size 150*150*150mm^3 and 6 cubes of size 70*70*70mm^3 for the compressive test of concrete and mortar respectively, 30 cylinders of size 150*300mm, and 6 cylinders of size 100*200mm for splitting tensile strength test of concrete and mortar respectively, and 39 cylinders of size 150*300mm for pull out test has been cast.

Aggregate size

Five different coarse aggregate sizes are chosen for the experiment from the ASTM C33 Gradation requirement of coarse aggregates as shown in Table 3.7[38].

- ✓ No. 467(37.5 to 4.75 mm)
- ✓ No. 56(25 to 9.5 mm)
- ✓ No. 67(19 to 4.75 mm)
- ✓ No. 7(12.5 to 4.75 mm)
- ✓ No. 89(9.5 to 1.18 mm)

Table 3.7. Grading Requirements for Coarse Aggregates

Size Number	Nominal Size (Sieves with Square Openings)	Amounts Finer than Each Laboratory Sieve (Square-Openings), Mass Percent													
		100 mm (4 in.)	90 mm (3½ in.)	75 mm (3 in.)	63 mm (2½ in.)	50 mm (2 in.)	37.5 mm (1½ in.)	25.0 mm (1 in.)	19.0 mm (¾ in.)	12.5 mm (½ in.)	9.5 mm (⅜ in.)	4.75 mm (No. 4)	2.36 mm (No. 8)	1.18 mm (No. 16)	300 µm (No.50)
1	90 to 37.5 mm (3½ to 1½ in.)	100	90 to 100	...	25 to 60	...	0 to 15	...	0 to 5	...	...	...	...	...	...
2	63 to 37.5 mm (2½ to 1½ in.)	...	...	100	90 to 100	35 to 70	0 to 15	...	0 to 5	...	...	...	...	...	...
3	50 to 25.0 mm (2 to 1 in.)	...	...	...	100	90 to 100	35 to 70	0 to 15	...	0 to 5	...	...	...	...	...
357	50 to 4.75 mm (2 in. to No. 4)	...	...	...	100	95 to 100	...	35 to 70	...	10 to 30	...	0 to 5	...	...	...
4	37.5 to 19.0 mm (1½ to ¾ in.)	...	...	...	...	100	90 to 100	20 to 55	0 to 15	...	0 to 5	...	...	...	...
467	37.5 to 4.75 mm (1½ in. to No. 4)	...	...	...	...	100	95 to 100	...	35 to 70	...	10 to 30	0 to 5	...	...	...
5	25.0 to 12.5 mm (1 to ½ in.)	...	...	...	...	...	100	90 to 100	20 to 55	0 to 10	0 to 5	...	...	...	...
56	25.0 to 9.5 mm (1 to ⅜ in.)	...	...	...	...	...	100	90 to 100	40 to 85	10 to 40	0 to 15	0 to 5	...	...	...
57	25.0 to 4.75 mm (1 in. to No. 4)	...	...	...	...	...	100	95 to 100	...	25 to 60	...	0 to 10	0 to 5	...	...
6	19.0 to 9.5 mm (¾ to ⅜ in.)	...	...	...	...	...	...	100	90 to 100	20 to 55	0 to 15	0 to 5	...	...	...
67	19.0 to 4.75 mm (¾ in. to No. 4)	...	...	...	...	...	...	100	90 to 100	...	20 to 55	0 to 10	0 to 5	...	...
7	12.5 to 4.75 mm (½ in. to No. 4)	...	...	...	...	...	...	...	100	90 to 100	40 to 70	0 to 15	0 to 5	...	...
8	9.5 to 2.36 mm (⅜ in. to No. 8)	...	...	...	...	...	...	...	...	100	85 to 100	10 to 30	0 to 10	0 to 5	...
89	9.5 to 1.18 mm (⅜ in. to No. 16)	...	...	...	...	...	...	...	...	100	90 to 100	20 to 55	5 to 30	0 to 10	0 to 5
9[A]	4.75 to 1.18 mm (No. 4 to No. 16)	...	...	...	...	...	...	...	...	...	100	85 to 100	10 to 40	0 to 10	0 to 5

[A] Size number 9 aggregate is defined in Terminology C125 as a fine aggregate. It is included as a coarse aggregate when it is combined with a size number 8 material to create a size number 89, which is a coarse aggregate as defined by Terminology

3.4. Methods

The methods applied to achieve the objectives are elaborated in this section.

Mix Design

The mix design is accomplished using ACI 211.1-91 standard procedure[39]. Specified C-25 Concrete was designed. The quantity of each ingredient is summarized in Table 3.8. Detailed calculation is presented in appendix C.

Table 3.8. Quantity of Material Required for Concrete

No	**Material**	**Weight of material (kg/m^3)**
1.	Water	211.62
2.	Cement	386
3.	Coarse aggregate	1078.01
4.	Fine aggregate	722.99

Mortar mix design

The mixture ratio of mortar is determined by investigating the previous studies and different trial mix, the mortar mix was designed using ASTM C 109[40] recommendation. The quantity of each ingredient is summarized in Table 3.9.

Table 3.9. Quantity of Material Required for Mortar

No.	**Material**	**Weight of material (kg/m^3)**
1.	Water	257.65
2.	Cement	515.3
3.	Fine aggregate	1366.7

Table 3.10. Mixtures Notation

No.	Mix notation	Description
1.	CA37.5	Concrete mixes containing coarse aggregate sizes of 37.5mm
2.	CA25	Concrete mixes containing coarse aggregate sizes of 25mm
3.	CA19	Concrete mixes containing coarse aggregate sizes of 19mm
4.	CA12.5	Concrete mixes containing coarse aggregate sizes of 12.5mm
5.	CA9.5	Concrete mixes containing coarse aggregate sizes of 9.5mm
6.	M1	Mortar mix with an embedment length of 70mm
7.	M2	Mortar mix with an embedment length of 150mm
8.	M3	Mortar mix with an embedment length of 200mm
9.	M4	Mortar mix with an embedment length of 250mm

3.5. Specimen Preparation

The pull-out specimens were cast using cylindrical samples (300*150mm), 16 mm and 14mm deformed bar was arranged vertically in the center of a concrete specimen.

Strain gauge

Within bonded regions when recording the local strain, due to physical damage of strain gauges applying surface-mounted method result in high failure rates. To tackling such a problem near-surface-mount methods employed for installing strain gauges, to protect the gauges from damage during both specimen preparation and testing. The local cross-section of the steel bar was modified slightly to enable the strain gauges to be positioned just below the surface of the ribbed bar. The strain gauges were attached inside grooves carefully to protect direct friction from the concrete destructing the wire and strain gauges connection during the process of concrete casting and bar slip. The longitudinal rib of the bar has been removed to attach strain gauges, Figure 3.5.

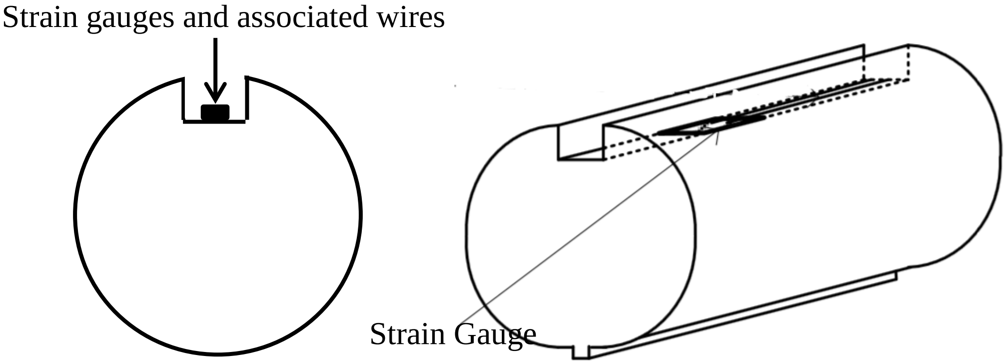

Figure 3.5. Strain gauges mounted inside of a groove

Figure 3.6. Longitudinal grooved deformed bars and application of the strain gauge on the bar

To allow the local strain to be measured continuously along the length of the bar during the pull-out test a total of three or four of the strain gauges were attached to the 150 mm length of each of the reinforcement bars bonded in the concrete. The steel reinforcing bar had one groove 3 mm wide by 3.5 mm deep machined along its sides. The grooves run 30 mm in the length along one side of the bar. Moreover, Foil strain gauges (series F, FLAB – 3 – 11 –

3LJB – F) having a Gauge length of 3mm were mounted in the longitudinal groove cut into the surface of the bar (near-surface-mount) at an interval of 5 cm for CA25-1 and M3 -1 for the remaining specimen at the interval of 7.5 cm to measure strain distribution along an embedded bar. Also, Strain Gauges Type PL-60-11-3LJCT-F having a Gauge length of 60mm were attached to the surface Along with a concrete specimen two diametrically opposite strain gauges were attached, the strain was obtained from the average value of these two concrete strain gauges. The steel strain gauges were used to measure the strain in the reinforcement bar and the typical values for the strain are often expressed in micro-strain units. Strain gauges were used to measure changes of the local strain during the experimental pull-out test. It should be noted that the gauges and related connecting wires placed in the groove were waxed to help prevent water and cement paste from entering during the production of the test specimens as shown in Figure 3.7.

Figure 3.7. Installation of strain gauges and sealed by wax

Pull out test specimens geometry

The pull-out tests were conducted with 150 mm diameter of a concrete cylinder (300 mm *150 mm) with centrally embedded 16 mm and 14 mm deformed bar of 1000 mm of total length to enable the gripped end of the bar to be secured, by a mechanical grip arrangement to the loading machine. The loaded end was long enough (700 mm = 1000 mm -300 mm) to allow for pull-out testing and the slip was measured using transducers at the free end. For some specimen, the embedment length of the rebar was planned to $5d_b$(70mm, 5*14mm) to have pullout failure as recommended by RILEM/CEB/FIP[41]. This short embedment length also allowed a uniform bond-stress distribution to be assumed. the remaining portion of the bars from the loaded end and free end was covered with a plastic tube to keep the bar from bonding with the concrete to achieve the desired development lengths. The ends of the plastic tubes were sealed with wax and also surrounded by plastic tape. The embedment length was also varied from 150mm up to 250 mm, to study the embedment length effect on bond strength of reinforced concrete, and strain distribution. An unbounded length of 75mm up to 25mm was reserved to eliminate the effect of the concrete edge during the loading process as shown in Figures 3.8(a) and (b).

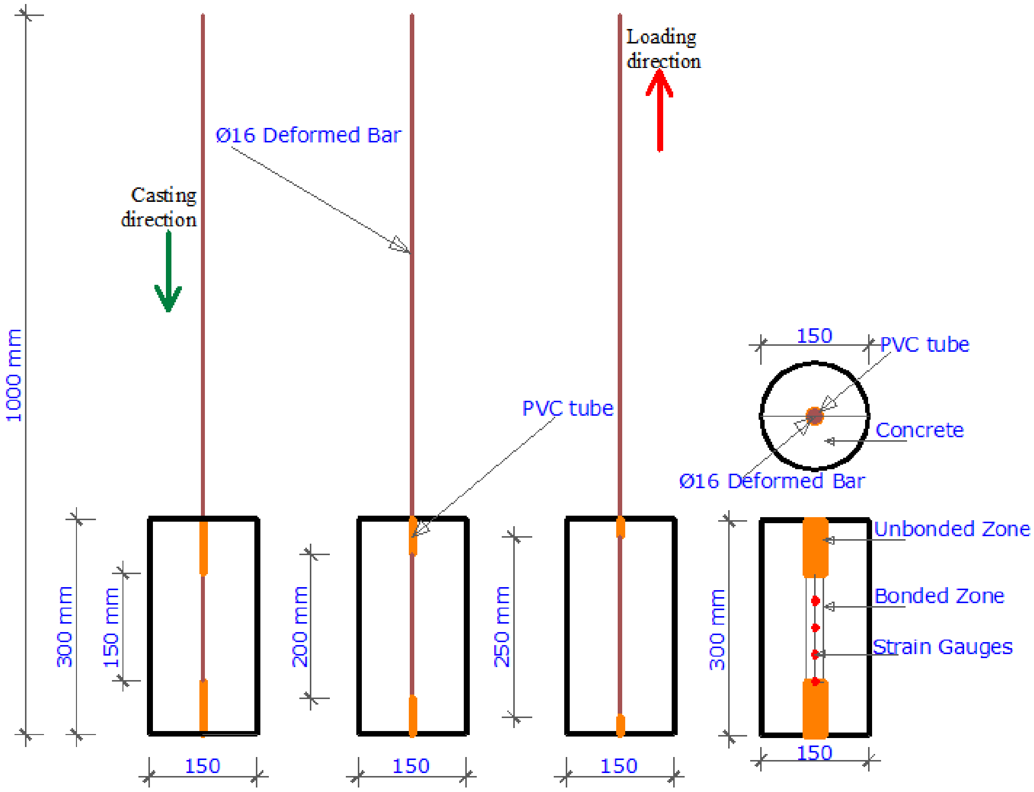

(a) (b) (c)

Figure 3.8.(a) Pull-out Specimens test details, Ø16mm (a). l_d=150mm (b). l_d=200mm, and (c). l_d=250mm.

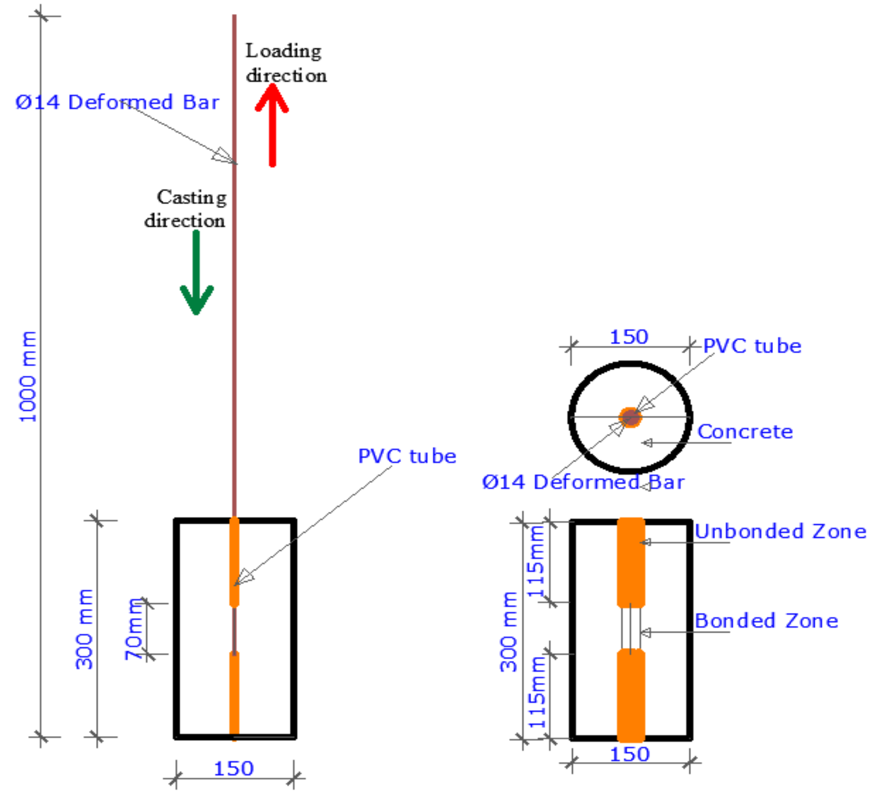

Figure 3.8. (b) Pull-out Specimens test details Ø14 mm, l_d = 70mm

As listed in Table 3.11, five types of Aggregate size served as the main variables for this study. All specimens were fabricated according to ASTM C234[26] and all the specimens had the same concrete cover-to-bar diameter ratio (C/d_b = 4.86) for those who have $5d_b$ (70mm)embedment length.

Table 3.11 Description of test specimens

Specimen	Cover (mm)	Bar Diameter (mm)	Embedment length (mm)
CA37.5	68	14	70
CA25			
CA19			
CA12.5			
CA9.5			

Concretes mix

All concretes were mixed in the laboratory using the mixer shown in Figure 3.9. Making and curing concrete test specimens in the laboratory was carried out according to ASTM C192[42]. The coarse aggregate was added to the mixer first followed by cement and fine aggregate, and then it was dry blended. Two-thirds of water was added and the mixing was continued for an additional minute. The remaining water is then added. The ingredients were thoroughly mixed in a mixer machine till uniform consistency was achieved.

Figure 3.9. Mixing Concrete

Slump tests of fresh concrete were done immediately after mixing to check the workability of concrete. The slump of every freshly mixed concrete is measured according to ASTM C-143[43].

Figure 3.10. Measuring Slump of Fresh Concrete

Fresh concrete was cast into a slump test cone were compacted per batch to determine its workability before being cast into the concrete cube molds. Before casting, machine oil was smeared on the inner surfaces of the molds and the bar was carefully installed as shown in Figure 3.11, to keep its center alignment. Finally, concrete was poured into the mold and compacted thoroughly and to ensure a proper consolidation, a table vibrator was used. After 24hrs the concrete specimens were taken out of their molds and put in a water tank for curing as shown in Figure 3.13 until the test date.

Figure 3.11. Oil paint concrete mold

Figure 3.12. Concrete Specimen after cast

Figure 3.13. Curing Concrete Specimens

3.6. The Test Set Up and Instrumentation

Pull-out testing

Figure 3.14. Specimen preparation for test and strain gauge arrangement

The instrumentation was mainly designed to capture the Bond stress-slip of the test specimens. The projected reinforcing bar passed through the center hole jack. It was gripped by the upper jaws of the testing machine. The load was applied by a center hole jack testing machine with a capacity of 130 kN and continuous monitoring of the applied load was done through the use of a center hole load cell as shown in Figure 3.15. Transducers were used to measure the free end slip of the bar during the experimental test. The strain gauges and transducers were connected to a data logger. The experimental data were recorded using video and the experiment result was retrieved through a USB flash disk.

Figure 3.15. The test set up

Figure 3.16. Datalogger

Testing Method

Compressive Strength Test

After the specimens were taken out from the curing tank just before the test, the concrete was surface dried and tested according to ASTM C39[44], weighed, and tested at seven and twenty-eight days with the Universal Testing Machine. The load was applied gradually with the rate of loading of 0.28MPa/sec until the failure stage and capacity of 3000kN. Three cylinders of each mix were tested for compressive strength at seven and twenty-eight day's concrete age. the detailed results of the compressive strength test are provided in appendix E.

Figure 3.17. Compressive Strength Test Setup

Splitting Tensile Strength Test

Tensile strength of concrete can be conducted using direct uniaxial and indirect methods such as flexural and splitting strength experiments. The splitting Tensile Strength method consists of applying a diametric compressive force along the length of a cylindrical concrete specimen at a rate of 689 to 1380 kPa/min until failure occurs (ASTM C-496-71). Three cylinder specimens of each concrete were tested for splitting tensile strength. At the concrete age of seven and twenty-eight days.

$$\sigma = \frac{2P}{\pi\, d_b\, l_d} \tag{3.1}$$

Where

P is the applied load at failure

d_b is the diameter of a cylinder

l_d is the length of the cylinder

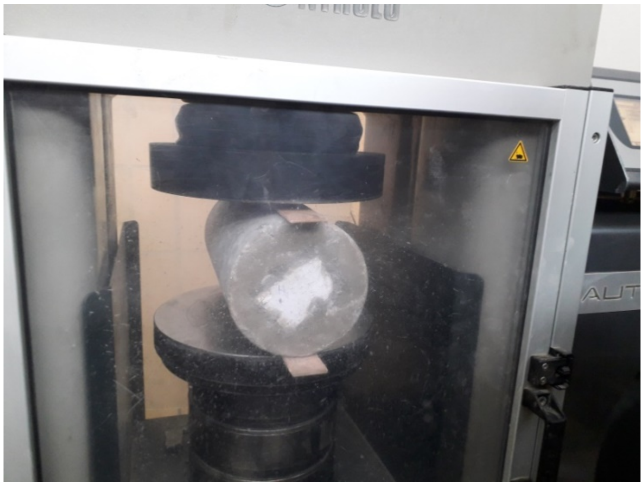

Figure 3.18. Splitting Tensile Strength Test Setup

Pullout Bond test

The pull-out test is used to determine the bond strength of concrete and steel by measuring the force required to pull the bar inserted in the concrete specimen. The load was applied by a center hole jack testing machine with a capacity of 130 kN. Three-cylinder specimens of each concrete were cast for pullout embedded with 14mm and 16mm diameter bars to test the bond strength.

Figure 3.19. Pullout Test Setup

4. RESULT AND DISCUSSION

4.1. Introduction

This chapter comes up with a summary of all experimental test results accompanied by the discussion that will be presented; the finding of an experimental program addresses the fresh and hard properties of concrete followed by the Bond investigations. The results found are discussed thoroughly concerning the previous work and internationally accepted standards.

4.2. Fresh Concrete Properties

Slump test

To check the workability of fresh concretes, a slump test is performed. Slump tests conducted for each concrete mix are presented below. Table 4.1 shows the results of the slump test.

Table 4.1 Average Slump Value for Each Mix

Mix notation	Average Slump Value (mm)
CA-37.5	93
CA-25	87
CA-19	81
CA-12.5	76
CA-9.5	67

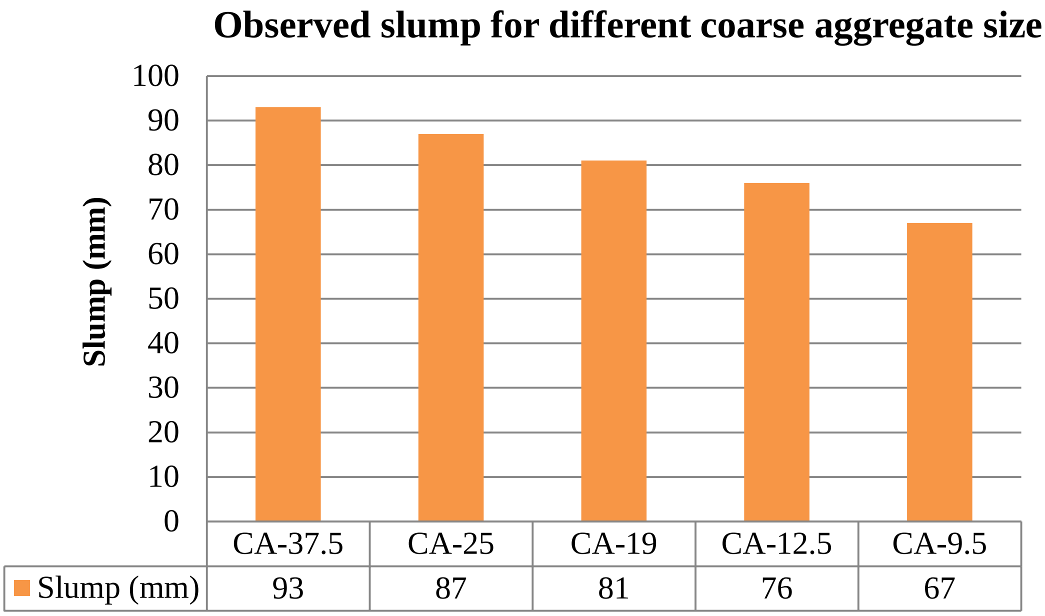

Figure 4.1. The observed slump for concrete mix

As indicated in Table 4.1, the loss of workability was noticed with decreasing the coarse aggregate size. The coarse aggregate size was proportional to the slump directly. the concrete became more workable As the slump increased[45].

4.3. Hardened Property of Concrete

To investigate the mechanical property of concrete for C-25 grade of concrete, compressive strength, and splitting tensile strength test at 7th, and 28th were tested. Table 4.2 and Table 4.3 shows the Compressive and Splitting Tensile Strength of the concrete used in the test samples.

Compressive Strength of Concrete

The compressive strength of concrete was tested and analyzed. The detailed results of the compressive strength test are provided in Appendix E. The average results are clearly described in Table 4.2.

Compressive strengths of all concrete are kept at the same level to study only the effect of coarse aggregate size on bond strength, but there is still an indication of an increase in concrete compressive strength when the Coarse aggregate size in concrete increases.

Table 4.2. Average compressive strength of concrete and mortar

No	**Mix notation**	**Average Compressive strength (MPa)**	
		7th day	**28th day**
1	**CA-37.5**	24.10	36.03
2	**CA-25**	23.01	35.45
3	**CA-19**	22.71	34.99
4	**CA-12.5**	22.40	34.05
5	**CA-9.5**	21.13	33.02
6	**Mortar**	22.92	35.80

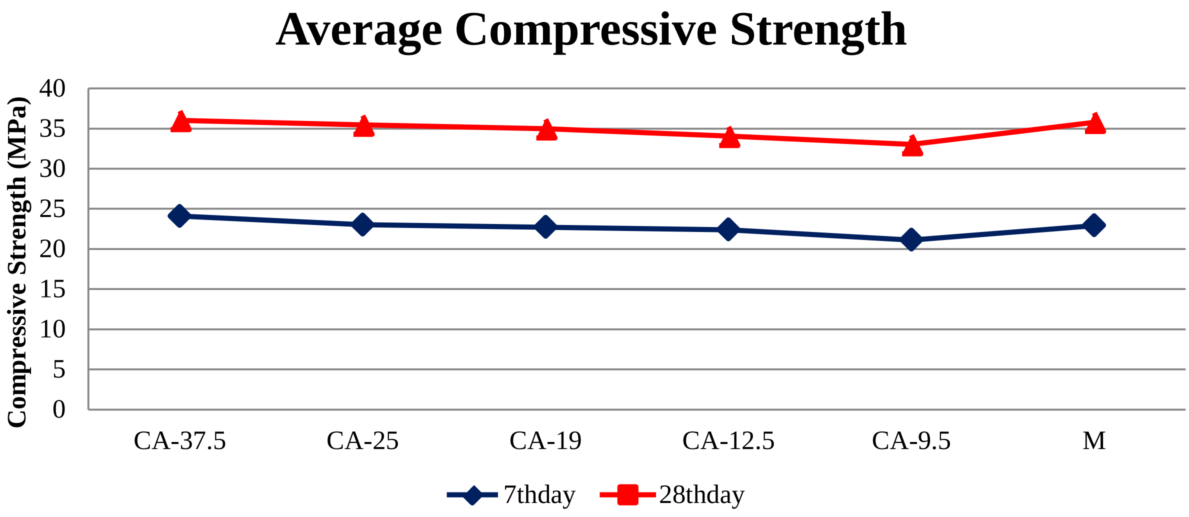

Figure 4.2. Average compressive strength of concrete and mortar

From Table 4.2 the compressive strength of the concrete decrease with decreasing the aggregate size. As it can be observed from 28th-day compressive strength for CA-19, CA-12.5, and CA-9.5 decrement in compressive strength by 1.34 %, 4.06 %, and 7.05 % respectively. Findings obtained in this study can be supported by A. Rabbani and T. Bruceroy [45], [46] who found the variation in compressive strengths may be due to the variations in the particular concrete batches between wetted surface areas. The wetted area of concrete batches of smaller aggregates is greater than larger aggregates. During the curing process, when the moistened area dries up, it leaves pores where micro cracks begin. Compared to large aggregates, this is the cause for the low compressive strength related to smaller aggregates. In general, increasing the coarse aggregate size leads to an increase of compressive strength of normal strength concrete. Very fine aggregate requires more water for the given consistency. With an increase in coarse aggregate size, the compressive strength of a concrete increases[47].

Splitting Tensile Strength of Concrete

The Splitting Tensile Strength test investigates concrete's tensile strength. This test is an indirect way of evaluating, using a cylinder, the tensile strength of concrete. The reason for an indirect test is due to the difficulty in applying uniaxial load on concrete. Because of the tension in the transverse direction, Specimen failure happens along its vertical diameter. The splitting tensile strength of concrete was tested and analyzed. The detailed results of the laboratory tests are given in Appendix E.

Table 4.3. Average splitting tensile strength of concrete and mortar

No	**Mix notation**	**Average Splitting Tensile Strength (MPa)**	
		7th day	**28th day**
1	**CA-37.5**	2.37	3.91
2	**CA-25**	2.35	3.88
3	**CA-19**	2.31	3.86
4	**CA-12.5**	2.28	3.79
5	**CA-9.5**	2.26	3.73
6	**Mortar**	2.36	3.89

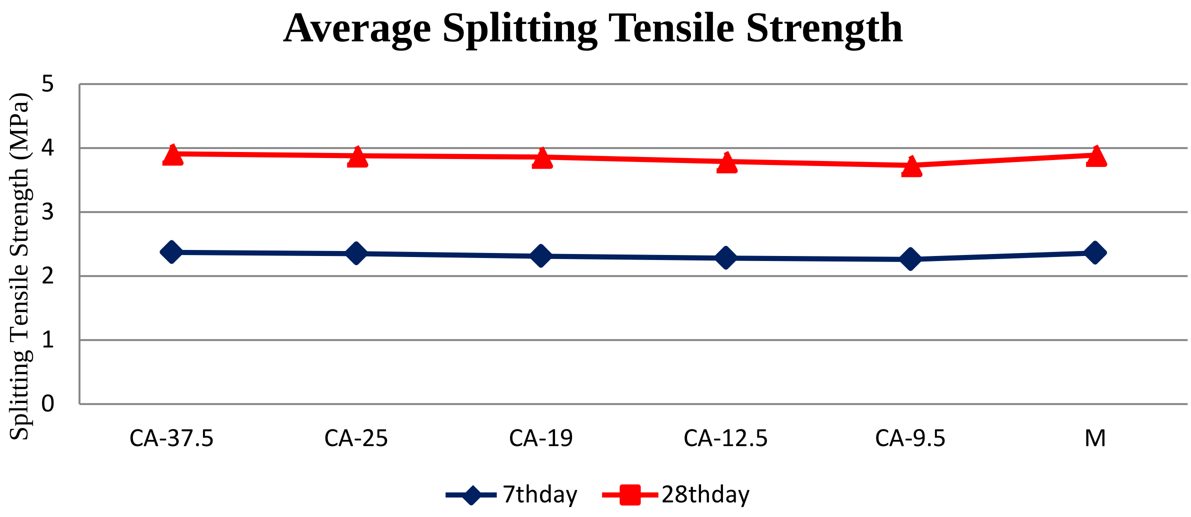

Figure 4.3. Average splitting tensile strength of concrete and mortar

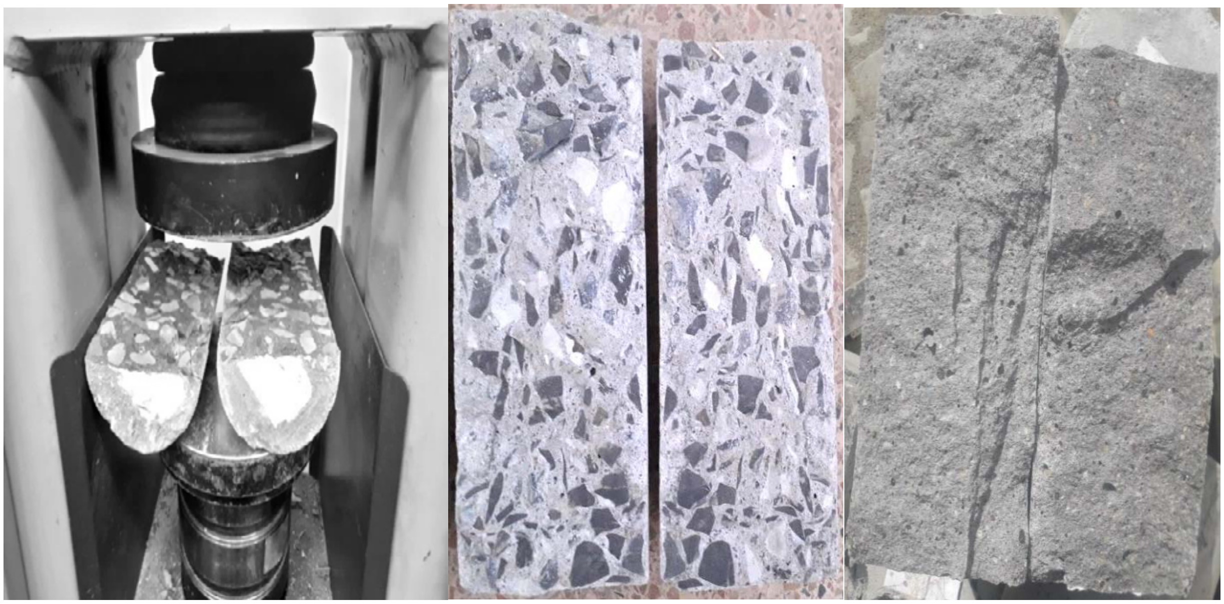

Figure 4.4. Tested specimens for splitting tensile strength

In the concrete mixture, the 25 mm coarse aggregate yields a slightly higher Splitting Tensile strength than the 9.5 mm coarse aggregate, although the difference is not significant. Concrete tensile strength is little influenced by coarse aggregate size. Accordingly, the Splitting Tensile Strength decreases with decreasing the coarse aggregate size likewise the compressive strength.

Concrete having a different coarse aggregate size, their mechanical properties was almost the same, which were intended only to research the effect of the coarse aggregate size on bond strength.

Pullout Strength

It is tolerable to consider uniform bond stress and slip in the case of small embedment length lengths. the average bond stress was calculated by dividing the pullout load by the bonded surface area of the bar, and the bond strength is given as:

$$\tau = \frac{p_u}{\pi\, d_b\, l_d} \tag{4.1}$$

Where

P_u is the maximum pull-out load,

d_b is the diameter of the bar, and

l_d is the embedded bar length.

Table 4.4 Pull out Test Result

Mix Notation	**Failure Load (kN)**	**Average Failure Load (kN)**	**Average Bond strength (Mpa)**	**Average Slip(mm)**	**Concrete Strain (‰)**		**Failure Mode**
					Right	**Left**	
CA-37.5$_1$	52.75	53.24	17.29	0.76	_	_	Pullout
$_2$	52.32				_	_	Pullout
$_3$	54.64				_	_	Pullout
CA-25$_1$	46.77	45.71	14.85	1.18	34.62	17.31	Pullout
$_2$	45.32				21.15	17.31	Pullout
$_3$	45.03				_	_	Pullout
CA-19$_1$	41.52	41.06	13.34	1.51	_	_	Pullout

2	42.21				_	_	Pullout
3	39.44				_	_	Pullout
CA-12.5$_1$	35.13	36.01	11.7	2.18	_	_	Pullout
2	36.91				_	_	Pullout
3	35.98				_	_	Pullout
CA-9.5$_1$	32.26	33.36	10.84	2.4	_	_	Pullout
2	33.87				_	_	Pullout
3	33.95				_	_	Pullout
M-1$_1$	27.15	28.04	9.11	3.03	33.65	23.08	Pullout
2	28.93				28.85	28.85	Pullout
3	28.04				_	_	Pullout

(-) No strain gauge attached, the concrete strain is at the failure load

Two concrete strain gauges were applied to the concrete, at the mid of the specimen. The strain was obtained from the average value of two concrete strain gauges.

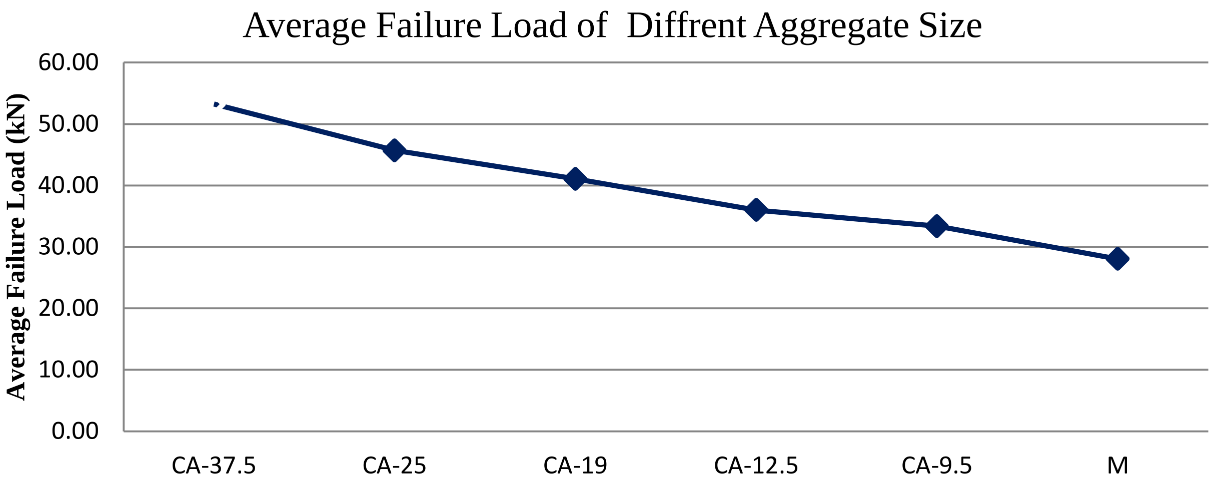

Figure 4.5. Average Failure Load of Different Aggregate Size

CA25 concrete mixture yields a higher failure load than CA9.5, as can be seen from Table 4.4. The mortar bond strength is significantly smaller than that of concrete. There is a noticeable difference with almost the same compressive strength, embedment length, and bar diameter having a bond strength of 45.71 and 28.04 MPa, respectively, which is about 38.65 percent. In the eighteen samples, the maximum load experienced was 54.64kN for those 5d_b(70 mm) embedment lengths. In the twenty-one samples, the highest load found was 126 kN for a sample with an embedment length of 150 mm, the detailed results of the split specimen are provided in appendix E.

In general, the failure modes of a sample depend on bar diameter, concrete strength, and concrete cover. Pull-out failure was dominant over splitting failures for those with smaller embedded lengths of 5d_b (70 mm), as shown in Figure 4.6(a), due to the availability of sufficient containment provided by the large concrete cover (68 mm). This form of failure occurs when the shear force produced from concrete exceeds the radial force of the steel bar, letting the reinforcement bar crush the concrete keys between each pair of lugs, and thus simply pulling out the reinforcement bar without any noticeable splitting of concrete. Splitting did not occur and the pull-out triggered the bond loss. As shown in Figure 4.6(b), specimens whose embedment length is 150 mm exhibited splitting failure, it is a pure concrete failure, the confining action created in concrete by the circumferential tensile forces was lesser than the radial force of the reinforcement bar. Therefore, on a steel-concrete interface, cracks are quickly propagated before reaching the external concrete surface.

Figure 4.6. Mode of failure: (a) pull-out failure; (b) splitting failure

Reinforcement mark remain on the concrete surface for pullout failure is smooth as the bar pullout easily. While for splitting failure since it is concrete failure there is remaining bar mark on concrete as shown in Figure 4.7.

Figure 4.7. Failure patterns, Remained marks of a bar in the tested concrete specimen : (a) pull-out failure; (b) splitting failure

Bond Strength-Slip

The bond strength-slip relationship of the samples tested is shown in Figure 4.8., which illustrates the bond strength as a function of free end slip for all the pull-out specimens.

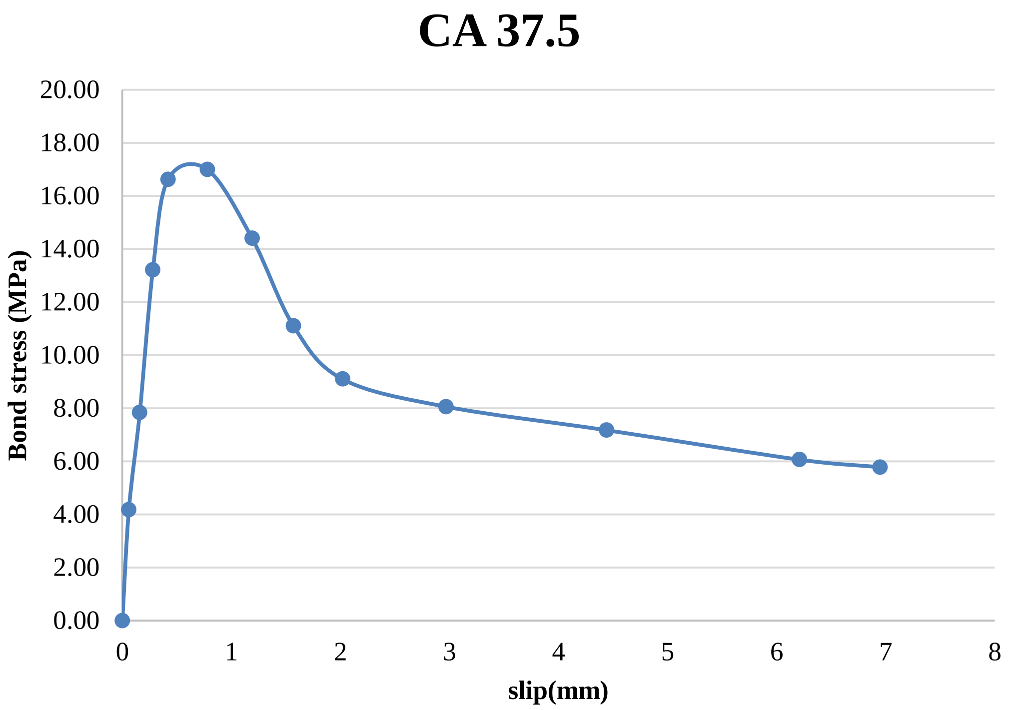
CA 37.5
20.00
18.00
16.00
14.00
12.00
10.00
8.00
6.00
4.00
2.00
0.00
Bond stress (MPa)
0
1
2
3
4
5
6
7
8
slip(mm)

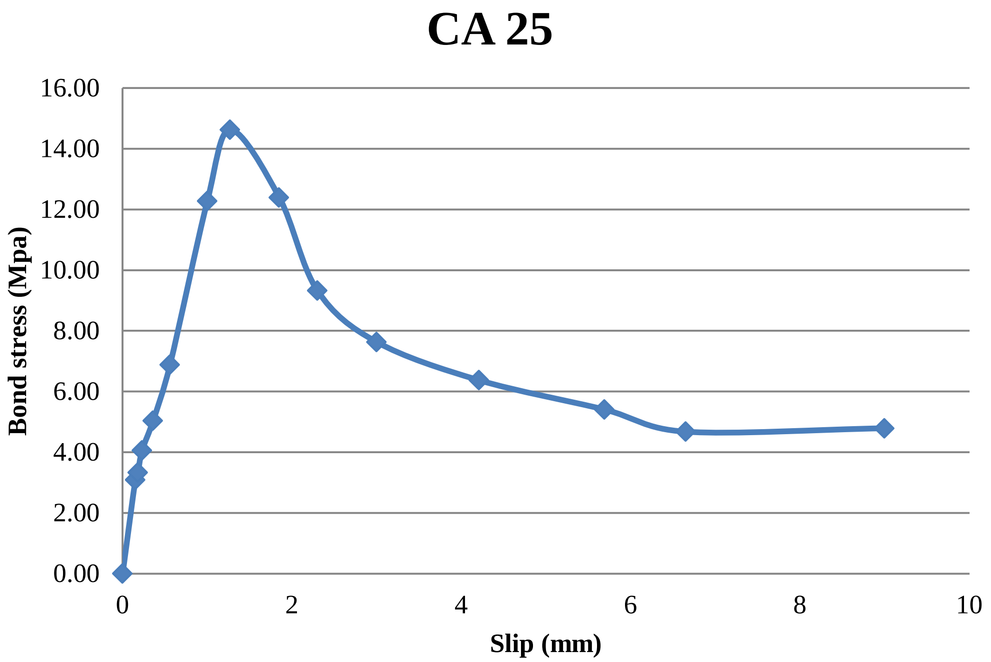
CA 25
16.00
14.00
12.00
10.00
8.00
6.00
4.00
2.00
0.00
Bond stress (Mpa)
0
2
4
6
8
10
Slip (mm)

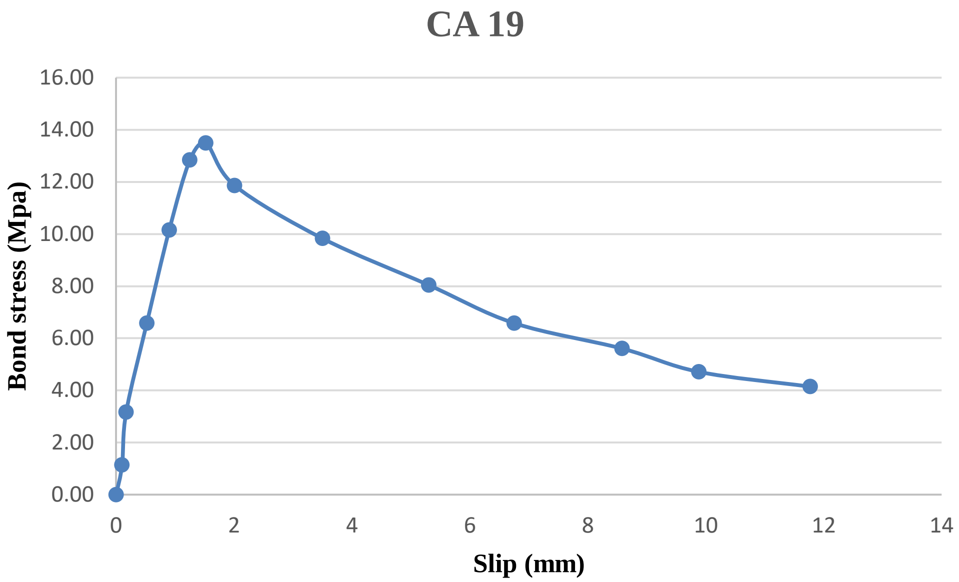
CA 19
Bond stress (Mpa)
16.00
14.00
12.00
10.00
8.00
6.00
4.00
2.00
0.00
0
2
4
6
8
10
12
14
Slip (mm)

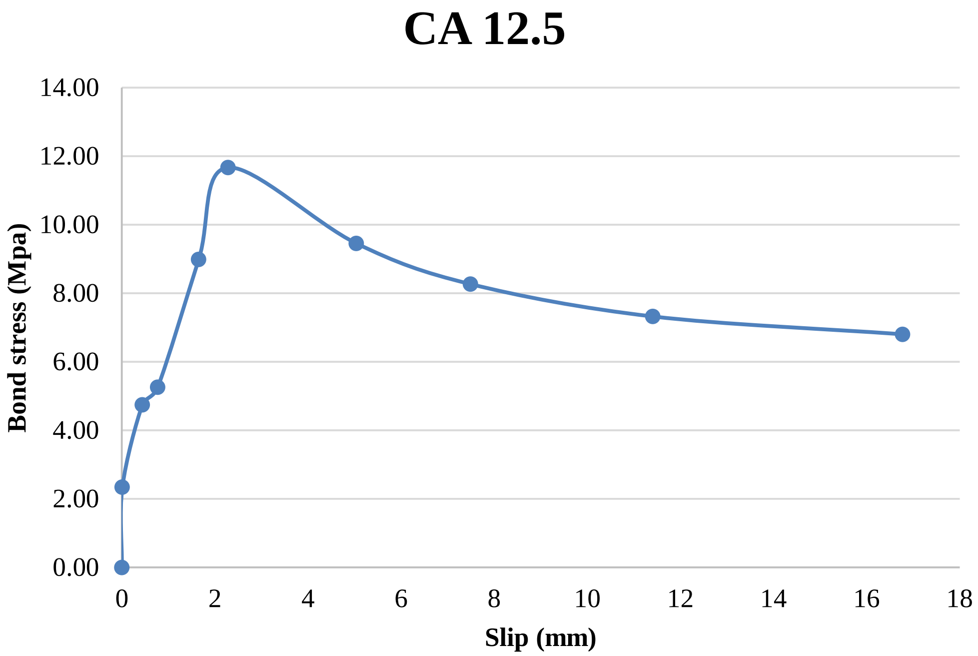
CA 12.5
Bond stress (Mpa)
14.00
12.00
10.00
8.00
6.00
4.00
2.00
0.00
0
2
4
6
8
10
12
14
16
18
Slip (mm)

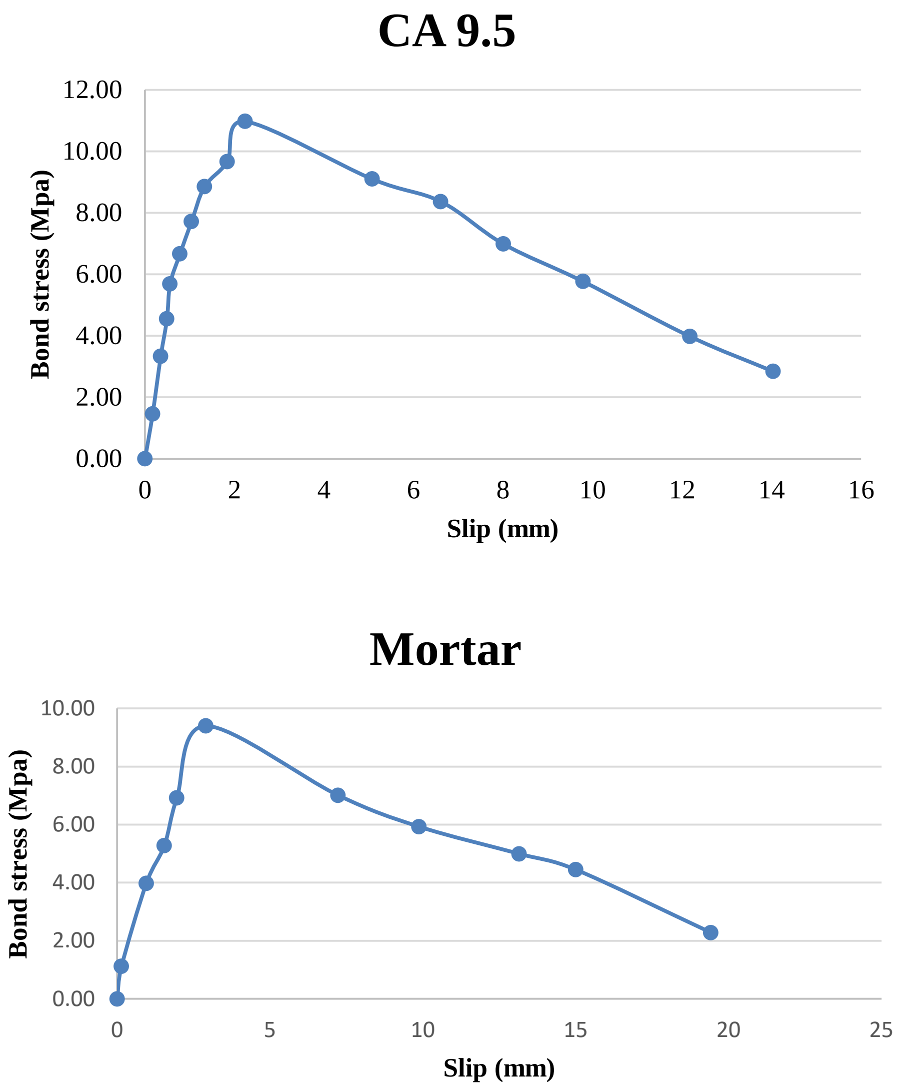

Figure 4.8. Bond stress versus slip curves of the pull-out specimens

The bond stress-slip behaviors of pullout specimens were obtained experimentally and the result of the bond stress was examined graphically as shown in Figure 4.8. To this end, almost similar shapes of the bond-slip curves were observed for concrete specimens, Before the maximum load occurred, the slip increased, and the maximum tensile load occurs at a small slip and then drops as the slip rises. With an increasing slip, the bond stress decreases. This may due to an uneven interface is gradually abraded to become flat. While for pure mortar the slip increases rapidly than the concrete specimens since there is no coarse aggregate it decreases in locking provided by aggregates to the pulled-out bar. The free end has no slip at the early loading in all pullout tests. With added loading increase to the extreme, the bar is pulled out quickly for pure mortar, the slippage at the free end began to increase rapidly.

The pullout bond-slip curve at the initial stage tended to be almost linear. The bond stress was growing rapidly and the slip was small. Followed by nonlinear curve rise, the bond stress increased to peak strength and the slip also increase. Finally, the bond-slip curve declines as the bond stress decreased, and the slip increases rapidly. As coarse aggregate size decreases bond strength decrease and the slip will increase this inter affects both strength and stiffness of structures.

4.4. Bond Strength Equations in Code Provisions and Empirical Equations

The experimental results for bond strength were compared with those calculated in the literature from different equations. Nine different equations were considered:

Several researchers have proposed equations for predicting the bond strength between steel reinforcement and surrounding concrete taking into account the main parameters such as compressive strength, bar diameter, embedment length, and concrete cover. It should be noted that the current code, as well as equations proposed by a different researcher, were just proposed based on the coarse aggregate size of 25mm not consider the different coarse aggregate sizes. The bond strengths obtained from the experimental tests have been compared to these equations and presented in Table 4.6.

Table 4.5. Parameter of the speciemns

Specimen	fc' (MPa)	d (mm)	L (mm)	C (mm)
CA37.5	36.03	14	70	68
CA25	35.45	14	70	68
CA19	34.99	14	70	68
CA12.5	34.05	14	70	68
CA9.5	33.02	14	70	68
Mortar	35.80	14	70	68

Table 4.6. Comparison of bond strength calculated from different equations with the experimental bond strength

Specimen	Failure Load (kN)	τ_{exp} (MPa)	Slip (mm)	Calculated bond strength (MPa)								
				Darwin et al	Orangun et al	Esfahani	Shima	CEB-FIP	AS 3600	JSCE code	ACI	CSA
CA37.5	53.24	17.29	0.76	13.14	12.85	14.69	9.82	15.01	8.52	3.05	3.15	3.94
CA25	45.71	14.85	1.18	13.03	12.74	14.57	9.71	14.88	8.45	3.02	3.13	3.91
CA19	41.06	13.34	1.51	12.95	12.66	14.47	9.63	14.79	8.40	3.00	3.11	3.88
CA12.5	36.01	11.70	2.18	12.77	12.49	14.28	9.45	14.59	8.28	2.94	3.06	3.83
CA9.5	33.36	10.84	2.4	12.58	12.30	14.06	9.26	14.37	8.16	2.88	3.02	3.77
Mortar	28.04	9.11	3.03	13.10	12.81	14.64	9.78	14.96	8.49	3.04	3.14	3.93

From comparison bond strength it can be seen that there is a general agreement with the experimental values for coarse aggregate 25mm but the proposed equation fails to predict for the other coarse aggregate size. Additionally, experimental bond stresses were less than the predicted value for coarse aggregate size less than 19mm.

Darwin et al. and Orangun et al

It can be observed that using the predicted values of bond strength recommended by [35] and [34] showed the closest results to the measured values. As shown in Table 4.6, the performance of predicted bond strengths by the previous equations [35], [34] generally show slight conservative results compared to the experimental results especially for coarse aggregate less than 19mm.

Esfahani & Rangan's

From Table 4.6, it can be noted that This equation [36] was less accurate as compared to [35] and [34]. The only factors considered in this equation were concrete cover, bar size, and compressive strength, while in addition to coarse aggregate Size the effect of embedment length was also not included in the equation.

CEB-FIP

CEB-FIP[31], gives overestimated values for specimens having a coarse aggregate size below 19mm compared to those experimentally obtained. concrete compressive strength is the only parameter that is used to estimate the maximum bond strength this is one of the main drawbacks of CEB-FIP and it does not take into account the effect of other important parameters such as bar diameter, concrete cover, coarse aggregate size, and embedment length. CEB-FIP is good in predicting bond strength values for coarse aggregate 25mm. The equations for CEB-FIP underestimated the bond shear stress of coarse aggregate 37.5mm but overestimated the bond strength for coarse aggregate less than 25mm.

Australian Standard

Table 4.6, indicate that all the bond strength predicted using this equation were less than smallest coarse aggregate size of experimentally obtained bond strength. In addition to different coarse aggregate size effect of length embedment is also not included by the equation forwarded by the Australian Standard [30] thus gives the same result at any length of the embedment.

ACI, CSA, JSCE code

In particular, the bond strength predicted using ACI, CSA, JSCE code and AS3600 equations show values significantly lower than those experimentally obtained because the equations of ACI and CSA code provisions are focused on the development lengths of reinforcement in the concrete structure. The other necessary parameter for estimating bond strength is not included here. In addition to the underestimation of the predictive equations, no factor for coarse aggregate size was considered in the code provisions and empirical equations. the predicted bond strength values that were calculated with the ACI code are about 23% lower than those predicted by the CSA code due to the bar diameter factor (In the ACI code, this factor is 1 for No. 7 and larger bars while in the CSA code, the factor is reduced from 1.0 to 0.8).

As shown in Table 4.6, the bond strength decreased as the aggregate size decreased for all the specimens, results indicate that as coarse aggregate size has a great contribution to the bond strength of reinforced concrete. The failure loads increased with the rising coarse aggregate size. When the size of the coarse aggregate decreases below 9.5mm, there is a drop in experimental bond strength results which may be due to a decrease in locking provided by small aggregates to the pulled-out bar. This drop is not empirically reflected both in the current code as well as in the equations proposed by different researchers that are used for bond strength prediction. Compared to smaller size aggregates, larger size aggregates may induce more resistance to bars by locking from the bar being pulled out, which is not considered in the empirical Equation. It can be concluded that even though these equations exhibited reasonable trends for predicting the bond strength of concrete, in addition to embedment length, concrete cover, bar diameter, and concrete strength more parameters such as different coarse aggregate sizes effect should have to be introduced in these empirical equations to improve the prediction accuracy of bond strength value and to better reflect the actual bond strength.

The comparison of all values is shown in Figure 4.9. The percentage of variations of equation values was calculated based on the experimental results. CEB-FIP fit well with the experimental values with less than 1% variation when 25mm coarse aggregate sizes are used. However, when the coarse aggregate size of 12.5mm was used, the variation was above 15%.

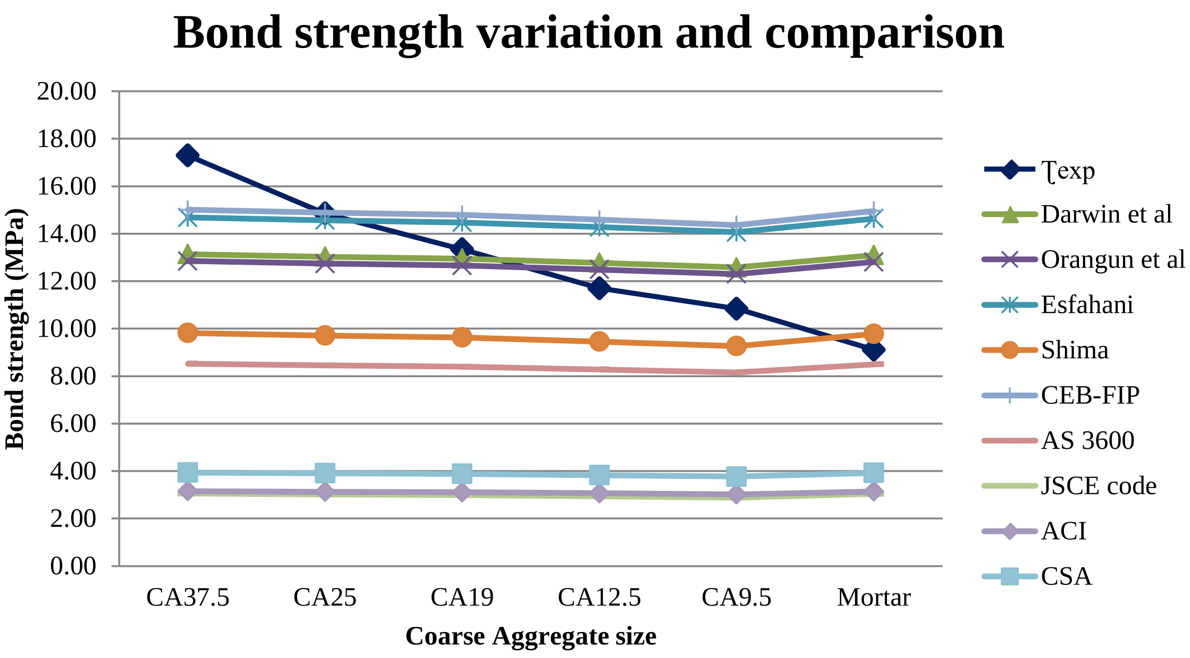

Figure 4.9. Bond strength variation and comparison

5. CONCLUSIONS AND RECOMMENDATIONS

5.1. Conclusions

Based on the experimental investigation results the following conclusion is drawn:

1. Coarse aggregate size has a great contribution to the bond strength of reinforced concrete.
2. The workability of concrete decreases with a decrease in aggregate size, workability (slump) was directly proportional to aggregate size.
3. There are decreases in experimental bond strength as the size of the coarse aggregate decreases, which may be due to a reduction in locking provided by small aggregates to a pulled-out bar.
4. The bond strength of pure mortar is significantly smaller than concrete (coarse aggregate size 25mm), which is about 38.65% that of concrete.
5. For pullout specimens, the free end has no slip at the initial loading. With added loading increase to the maximum, the bar pulled out rapidly for pure mortar, slipping at the free end began, and then quickly increased.
6. CEB-FIP for bond strength calculation works well for coarse aggregate size 25mm concretes but does not work sound when lower coarse aggregate sizes are used.
7. It is noticed that the splitting failure is the predominant type of failure observed in specimens for embedment length 150mm up to 250mm however for $5d_b$ pull-out failure was the predominant failure.
8. The compressive strength, and splitting tensile strength of concrete increase slightly with an increase in the coarse aggregate size used in concrete.

5.2. Recommendations

5.2.1. Recommendations from This Study

The following point's recommendations are forwarded based on the findings of the research:

Even though previously proposed equations exhibited reasonable trends for estimating the bond strength of concrete, the critical parameters, different coarse aggregate sizes effect should have to be introduced in the empirical equations to improve the accuracy of bond value and to better reflect the actual bond strength.

5.2.2. Recommendations for Further Study

Based on this study, the following aspects are suggested for further study:

Due to limitations in laboratory equipment, cylindrical specimens with centrally embedded deformed bar were being conducted. However real congested beam-column joint structural elements could be conducted to obtain a more comprehensive result.

An experimental program could be conducted to study the bond strength of large-scale pullout specimens, having a large cover and long embedment length.

REFERENCES

[1] P.Mehta and J.Monteiro, *Concrete Structure, Properties, and Materials, Prentice-Hall, Inc., Englewood Cliffs, NJ*. 1993.

[2] P.Tastani and J.Pantazopoulou, “Direct tension pull-out bond test: Experimental Results,” *Journal of Structural Engineering*, vol. 6, no. 136. pp. 731–743, 2009.

[3] ACI Committee, “Bond development of straight reinforcing bars in tension (ACI 408R-03),” *American Concrete Institute*. 2003.

[4] M. Behera, S. Bhattacharyya, A. Minocha, R. Deoliya, and S. Maiti, “Recycled aggregate from C & D waste & its use in the concrete – A breakthrough towards sustainability in construction sector : A review,” *Construction and Building Materials*, vol. 68. Elsevier Ltd, pp. 501–516, 2014.

[5] J. Xiao and H. Falkner, “Bond behavior between recycled aggregate concrete and steel rebars,” *Construction and Building Materials*, vol. 21, no. 2. pp. 395–401, 2007.

[6] S.Uma and A. Meherprasad, “Seismic Behavior of Beam-Column Joints in Reinforced Concrete Moment Resisting Frames,” *Department of Civil Engineering Indian Institute of technology Madras Chennai*, vol. 7. pp. 521–532, 2006.

[7] H. Shima, L. Chou, and H. Okamura, “Micro and Macro Models for Bond in Reinforced Concrete.,” *Journal of the Faculty of Engineering, University of Tokyo, Series B*, vol. 39, no. 2. pp. 133–194, 1987.

[8] K. Lundgren, “Bond between ribbed bars and concrete. Part 1: Modified model,” *Magazine of Concrete Research*, vol. 57, no. 7. pp. 371–382, 2005.

[9] C. Mahrenholtz, *Seismic Bond Model for Concrete Reinforcement and the Application to Column-to-Foundation Connections*. 2012.

[10] British.Standard, “Structural Use of Concrete.,” *BS 8110-11997*, vol. 4, no. 1, pp. 31–32, 1973.

[11] K. Wight and G. MacGregor, *Reinforced Concrete Mechanics and Design*, 5th ed. 2009.

[12] K. Maekawa, A. Pimanmas, and H. Okamura, “Nonlinear Mechanics of reinforced concrete,” *London, UK, Spon Press*, pp. 21–30, 2003.

[13] R. Eligehausen, P. Popov, and V. Bertero, “Local Bond Stress-Slip Relationships of

Deformed Bars Under Generalized Excitations," *in: proceeding of the 7th European Conference on Earthquake Engineering*, vol. 4, no. November. pp. 69–80, 1982.

[14] Z. Huang and B. Engstrom, "Experimental and analytical studies of the bond behavior of deformed bars in high strength concrete," *4th International Symposium on Utilization of High Strength/High Performance Concrete-BJP 96. Paris:* pp. 1115–1124, 1996.

[15] H. Kwak and S. Kim, "Bond-slip behavior under monotonic uniaxial loads," *Engineering Structures*, vol. 23, no. 3. pp. 298–309, 2001.

[16] S. Khalfallah, "Tension stiffening bond modeling of cracked flexural reinforced concrete beams," *Journal of Civil Engineering and Management*, vol. 14, no. 2. pp. 131–137, 2008.

[17] B. Lee and M. Mulheron, "Fluctuation of bond stress-slip behavior of deformed bar under displacement control," *Magazine of Concrete Research*, vol. 64, no. 10. pp. 863–875, 2012.

[18] T. Paulay, R. Park, and M. Priestley, "Reinforced concrete beam-column joints under seismic actions," *ACI structural journal*, vol. 75, no. 11. pp. 585–593, 1978.

[19] T. Paulay and M. Priestley, "Seismic design of reinforced concrete and masonry buildings," *ACI structural journal*, vol. 108, no. 5. pp. 616–621, 1992.

[20] J. Maguire, "An investigation to determine the effects that varying levels of corrosion have on the bond behavior for embedded reinforcement in high-strength concrete," *MENG, University of Surrey*. pp. 19–26, 2011.

[21] J. Lucini, "Laboratory-based investigation of the bond between steel and concrete," *MEng, University of Surrey*. pp. 31–44, 2011.

[22] R. Mains, "Measurement of the distribution of tensile and bond stresses along reinforcing bars," *ACI Journal Proceedings*, vol. 48, no. 11. pp. 225–252, 1951.

[23] R. Scott and P. Gill, "Shot-Term distributions of strain and bond stress along with tension reinforcement," *The Structural Engineer*, vol. 65, no. 2. pp. 39–48, 1987.

[24] J. Weathersby, "Investigation of bond-slip between concrete and steel reinforcement under dynamic loading conditions," *Ph.D., Louisiana State University*. pp. 193–212, 2003.

[25] RILEM TC, "Bond test for reinforcement steel. 2. Pull-out test, in RILEM (Ed.),

RILEM Recommendations for the Testing and Use of Constructions Materials,” *E & FN SPON*, pp. 218–220, 1994.

[26] ASTM C234, “Standard Test Method for Comparing Concretes based on the Bond Developed with Reinforcing Steel,” *Annual Book of ASTM Standards*, vol. 4, no. 2. 1991.

[27] Fib Bulletin 72, “Bond and anchorage of embedded reinforcement: Background to the fib Model Code for Concrete Structures 2010.” 2014.

[28] ACI Committee 318, “Building Code for Structural Concrete (318R–2008) and Commentary (318R–2008),” *American Concrete Institute, Farmington Hills, MI,*. 2008.

[29] CSA CAN3-A23.3, “Design of Concrete Structures,” *Canadian Standards Association, Rexdale, Ontario, Canada*, 2004.

[30] AS3600, “Australian Standard for Concrete Structures,” *Standards Australia, Sydney*, 1994.

[31] CEB-FIP, “CEB-FIP Model Code 2010,” *Fib Model Code for Concrete Structures*. 2010.

[32] JSCE, “Standard specifications for concrete structures: structural performance,” *Japan Society of Civil Engineers, Tokyo, Japan*, 2002.

[33] Ministry of Urban Development & Construction, “Design of Concrete Structures,” *ESEN 1992-1-1*, pp. 139–143, 2015.

[34] C. Orangun, J. Jirsa, and J. Breen, “Reevaluation of Test Data on Development Length and Splices.,” *ACI structural journal*, vol. 74, no. 3. pp. 114–122, 1977.

[35] D. Darwin, S. McCabe, E. Idun, and S. Schoenekase, “Development length criteria: bars not confined by transverse reinforcement,” *ACI structural journal*, vol. 89, no. 6. pp. 709–720, 1992.

[36] M. Esfahani and B. Rangan, “Bond between normal strength and high-strength concrete (HSC) and reinforcing bars in splices in beams,” *structural journal*, vol. 95, no. 3. pp. 272–280, 1998.

[37] ASTM C-125, “Standard Terminology Relating to Concrete and Concrete Aggregates,” *Annual Book of ASTM Standards*, vol. 04, no. 01. pp. 1–4.

[38] ASTM C-33-01, “Standard Specification for Concrete Aggregates,” *Annual Book of*

ASTM Standards, vol. 04, no. 02. pp. 1–8.

[39] ACI Committee 211, “Standard Practice for Selecting Proportions for Normal, Heavyweight, and Mass Concrete, ACI 211.1-91.” 1991.

[40] ASTM Committee, “ASTM C109/C109M-02. Standard Test Method for Compressive Strength of Hydraulic Cement Mortars,” *Annual Book of ASTM Standards*, vol. 04. pp. 1–6, 2002.

[41] RILEM/CEB/FIP., “Recommendations on reinforcement steel for reinforced concrete (RC 6, CEB News 73).” 1983.

[42] ASTM C 192/C 192M-02, “Standard Practice for Making and Curing Concrete Test Specimens in the Laboratory,” *Annual Book of ASTM Standards*, vol. 04. pp. 1–8, 2002.

[43] ASTM C-143, “Standard Test Method for Slump of Hydraulic-Cement Concrete,” *Annual Book of ASTM Standards*, vol. 04, no. 02. pp. 1–3, 2008.

[44] ASTM C 39/C 39M-03, “Standard Test Method for Compressive Strength of Cylindrical Concrete Specimens,” *Annual Book of ASTM Standards*, vol. 04, no. C. pp. 1–7, 2010.

[45] A. Rabbani, “Influence of the size of aggregates on the Compressive strength of concrete,” *International Journal of Engineering Development and Research*, vol. 5, no. 3. pp. 27–30, 2017.

[46] T. Bruceroy and S. Ndlangamandla, “The Effect of Aggregate Size on the Compressive Strength of Concrete,” *Journal of Agricultural Science and Engineering*, vol. Vol. 2 (6). pp. 66–69, 22-Dec-2016.

[47] S. Ajamu and J. Ige, “Effect of coarse aggregate size on the compressive behavior of geopolymer concrete,” *Journal of Engineering Research and Applications*, vol. 5, no. 1. pp. 67–75, 2015.

APPENDIX

Appendix A - Tests for Fine Aggregate

A-1: Sieve analysis results of fine aggregate

Sieve Size(mm)	Weight Retained (g.)	Percent Retained (%)	Cumulative Retained (%)	Cumulative Passing (%)	ASTM C 33 Standard passing range (%)
4.75	0	0	0	100	95-100
2.36	32	5	5	95	80-100
1.18	71	16	21	79	55-85
0.6	128	27	48	52	25-60
0.3	214	43	91	9	5-30
0.15	47	7	98	2	0-10
Pan	8	2	100	0	0

Fineness modulus = $\frac{\sum(\text{cumulative percent retained})}{100} = \frac{263}{100} = 2.63$

A-2: Moisture content of fine aggregate

Weight of original sample = 500g

Weight of original sample + weight of container=535g

Weight of container =35g

Weight of oven-dry sample =526.59g

Moisture content

$$= \frac{\text{original sample weight} - (\text{oven dry weight} - \text{Weight of container})}{(\text{oven} - \text{dry weight})} * 100\%$$

Moisture content = $\frac{500-(526-35)}{(526-35)} * 100\% = 1.71\%$

A-3: Specific gravity for fine aggregate

Weight of original sample=500g

Weight of water+ weight of pycnometer =1263g

Weight of sample+ water+ pycnometer =1763g

Weight of oven-dry sample =482.5g

Bulk specific gravity= $\frac{482.5}{1263+500-1565} = 2.44$

Bulk specific gravity (SSD basis) = $\frac{500}{1263+500-1565} = 2.53$

Apparent specific gravity= $\frac{482.5}{1263+482.5-1565}$=2.67

Absorption capacity=$\frac{500-482.5}{482.5} * 100$ =3.63%

Appendix B - Tests for Coarse Aggregate

B-1: Sieve analysis results of coarse aggregate

Sieve Size(mm)	Weight Retained (kg)	Percent Retained (%)	Cumulative Retained (%)	Cumulative Passing (%)	ASTM C 33 Standard passing range (%)
37.5	0	0	0	100	100
25	5.15	35.36	35.36	64.64	90-100
19	3.89	23.2	58.56	41.44	40-85
12.5	3.01	22.8	81.36	18.64	10-40
9.5	1.73	9.23	90.59	9.41	0-15
4.75	1.13	8.67	99.26	0.74	0-5
pan	0.09	0.74	100	0	0

Fineness modulus = $\frac{\sum(\text{cumulative percent retained})}{100} = \frac{365.13}{100} = 3.65$

B-2: Moisture content of coarse aggregate

Weight of original sample = 2000g

Weight of container= 425g

Weight of oven-dry sample = 2395g

$$\text{Moisture content} = \frac{\text{original sample weight} - (\text{oven dry weight} - \text{Weight of container})}{(\text{oven} - \text{dry weight})} * 100\%$$

Moisture content $= \frac{2000-(2395-425)}{(2395-425)} * 100\%$ = 1.52%

B-3: Specific gravity for coarse aggregate

Measurement Oven Dry (OD), Wt. of Sample = 4879.3g (A)

Measurement in the air (SSD), Wt. of Sample = 4975g (B)

Measurement soaked in water (Submerged), Wt. of Sample = 3241g (C)

Relative Density (Specific Gravity) OD = $\frac{A}{B-C} = \frac{4879.3}{4975-3241} = 2.81$

Relative Density (Specific Gravity) SSD = $\frac{B}{B-C} = \frac{4975}{4975-3241} = 2.87$

Apparent Specific Gravity: = $\frac{A}{A-C} = \frac{4879.3}{4879.3-3241} = 2.98$

Absorption Capacity (%): = $\frac{B-A}{A} * 100 = \frac{4975-4879.3}{4879.3} = 1.96\%$

Appendix C - Mix Design

C-1: Mix Design for C-25

Step 1: - Material Data

No.	Test Description	Cement	Coarse Aggregate	Fine Aggregate
1.	Specific Gravity	3.15	-	-
2.	Bulk Density (Unit Weight)	-	1569.16kg/m^3	1516.3kg/m^3
3.	Moisture content:	-	1.52%	1.71%
4.	Water absorption	-	1.96%	3.63%
5.	Bulk Specific Gravity (SSD basis)	-	2.87g/cm^3	2.53g/cm^3
6.	Silt content	-	-	0.37%
7.	Fineness Modulus (FM)	-	3.65	2.63

Step 2: - Choice of Slump

According to ACI 211 Table: A1.5.3.1 the recommended slump To address more frequent constructions of concrete we considered Beams, Columns, and reinforced walls whose slump ranges between 25 to 100mm, maximum slump= 100mm, and minimum slump= 25mm.

Step 3: - Choice of Max size of Aggregate

Coarse aggregates =25mm

Step 4: - Estimation of Mixing water & Air content

Consider non-air-entrained concrete, from table 2 of ACI standards, for non-air entrained and slump of 75-100, the water in 1m³ of concrete is 193 Kg.

Step 5: - Selection of Water-Cement ratio (W/C)

W/C = 0.5

Step 6: - Calculation of Cement content

Cement content (Kg) per cubic meter of concrete is:- $\frac{Wm}{W/C} = \frac{193}{0.5} = 386kg/m3$

Step 7: - Estimation of Coarse aggregate (CA) content

For FM = 2.63 of Fine aggregate and Maximum Size of aggregate

The volume of dry-rodded aggregate per cubic meter of concrete from the ACI Table is 0.687

Mass of Coarse aggregate, CA = Volume * Dry rodded unit mass= 0.687*1569.16= 1078.01 Kg

Step 8: - Estimation of fine aggregates content

Content of fine aggregate (F.A) = unit weight of concrete – (C.A + cement + water)

From table 5 the unit weight of fresh concrete corresponding to max. The aggregate size of 25mm and non-air entrained is 2380kg/m^3.

Fine aggregate content = [2380 – (1078.01+386+193)] = 722.99kg/m^3

Step 9: - Adjustment for aggregate moisture

If absorption capacity is greater than the moisture content of aggregate, we need to add water up to its moisture capacity.

C.A $_{water}$ = 1.96 - 1.52 = 0.44%

F.A $_{water}$ = 3.63 – 1.71 = 1.92%

Total water required = 193 + [1078.01 $*$ 0.44%+ 722.99 $*$ 1.92%] = 211.62Kg/m3

The estimated ingredients for a meter cube of concrete are, therefore, summarized as follows.

No	Material	Weight of material (kg/m^3)
1.	Water	211.62
2.	Cement	386
3.	Coarse aggregate	1078.01
4.	Fine aggregate	722.99

Appendix D - Mechanical Properties of Reinforcement Bar

Specimen No	**Diameter**		**Average Diameter (mm)**	**Area (mm2)**	**Yield load(kN)**	**Failure load(kN)**	**Elongation (%)**	**Mass/length(kg/m)**	**Length (cm)**	**Yield Strength (Mpa)**	**Ultimate strength (Mpa)**	**Average Yield Strength (Mpa)**	**Average Ultimate strength (Mpa)**
	D1, (mm)	D2, (mm)											
14-1	13.4	14.69	14.045	154.93	84.9	101.3	22.9	1183.1	101	547.99	653.85	549.61	671.97
14-2	13.45	14.68	14.065	155.37	85.7	105.6	22.5	1184.2	100	551.58	679.66		
14-3	13.47	14.67	14.07	155.48	85.4	106.1	22.4	1185.9	100	549.26	682.40		
16-1	15.67	16.94	16.305	208.8	131.2	143.8	22.9	1653.3	106	628.35	688.70	632.61	711.13
16-2	15.64	16.95	16.295	208.54	132	148.1	22.7	1654.4	103	632.96	710.16		
16-3	15.6	16.96	16.28	208.16	132.5	152.9	22.6	1657.2	101	636.53	734.53		

Appendix E - Test Results for Compressive, Splitting Tensile, and Pullout Strength

E-1: Test Results for Compressive Strength

Mix Notation	Test Age (Days)	Mass (g)	Failure Load (KN)	Compressive Strength (MPa)	Average Compressive Strength (Mpa)
CA-37.5	7	8465	551.03	24.49	24.10
		8269	550.80	24.48	
		8347	525.15	23.34	
	28	8475	796.88	35.42	36.03
		8569	832.10	36.98	
		8497	803.23	35.70	
CA-25	7	8205	530.55	23.58	23.01
		8069	512.78	22.79	
		8120	509.63	22.65	
	28	8290	785.41	34.91	35.45
		8357	811.85	36.08	
		8294	795.35	35.35	
CA-19	7	7952	520.20	23.12	22.71
		7875	513.45	22.82	
		7876	499.05	22.18	
	28	8127	788.47	35.04	34.99
		8074	774.36	34.42	
		8151	799.16	35.52	
CA-12.5	7	7828	512.91	22.80	22.40
		7694	497.23	22.10	
		7765	502.13	22.32	
	28	8011	761.11	33.83	34.05
		8029	777.06	34.54	
		7958	760.19	33.79	
CA-9.5	7	7636	470.70	20.92	21.13
		7594	464.40	20.64	
		7693	491.18	21.83	
	28	8117	738.95	32.84	33.02
		7974	733.21	32.59	
		8188	756.99	33.64	
M	7	735	510.08	22.67	22.92
		736	512.33	22.77	
		737	524.93	23.33	
	28	758	806.18	35.83	35.80
		757	819.68	36.43	
		755	790.65	35.14	

E-2: Test Results for Splitting Tensile Strength

Mix Notation	Test Age (Days)	Mass (g)	Failure Load (KN)	Compressive Strength (MPa)	Average Compressive Strength (Mpa)
CA-37.5	7	13289	170.45	2.41	2.37
		13125	166.14	2.35	
		13158	165.16	2.34	
	28	13654	280.18	3.96	3.91
		13362	271.38	3.84	
		13470	276.69	3.91	
CA-25	7	12882	168.84	2.39	2.35
		12785	164.31	2.32	
		12792	164.66	2.33	
	28	13225	278.61	3.94	3.88
		12959	269.77	3.82	
		13093	274.72	3.89	
CA-19	7	12387	159.05	2.25	2.31
		12540	167.92	2.38	
		12473	163.23	2.31	
	28	12758	276.00	3.90	3.86
		12796	276.84	3.92	
		12589	265.60	3.76	
CA-12.5	7	12289	154.13	2.18	2.28
		12407	166.57	2.36	
		12325	161.84	2.29	
	28	12564	270.48	3.83	3.79
		12459	258.61	3.66	
		12770	273.87	3.87	
CA-9.5	7	12110	156.11	2.21	2.26
		12297	161.63	2.29	
		12300	160.78	2.27	
	28	12741	271.19	3.84	3.73
		12549	257.40	3.64	
		12578	262.71	3.72	
M	7	3396	74.84	2.38	2.36
		3388	74.27	2.36	
		3387	72.86	2.32	
	28	3342	122.67	3.90	3.89
		3435	121.98	3.88	
		3408	121.65	3.87	

Appendix E-3: Pull out Test Results

Mix Notation	**Failure Load (kN)**	**Average Failure Load (kN)**	**Bond Strength (MPa)**	**Average Bond Strength (MPa)**	**Slip (mm)**	**Average Slip (mm)**	**Concrete Strain (‰)**		**Failure Mode**
							Right	**Left**	
CA-37.5$_1$	52.75	53.24	17.13	17.29	0.8	0.76			Pull out
$_2$	52.32		16.99		0.78				Pull out
$_3$	54.64		17.75		0.71				Pull out
CA-25$_1$	46.77	45.71	15.19	14.85	1.07	1.18	34.62	17.31	Pull out
$_2$	45.32		14.72		1.19		21.15	17.31	Pull out
$_3$	45.03		14.63		1.27		_	_	Pull out
CA-19$_1$	41.52	41.06	13.49	13.34	1.52	1.51	_	_	Pull out
$_2$	42.21		13.71		1.43		_	_	Pull out
$_3$	39.44		12.81		1.57		_	_	Pull out
CA-12.5$_1$	35.13	36.01	11.41	11.70	2.28	2.18	_	_	Pull out
$_2$	36.91		11.99		2.07		_	_	Pull out
$_3$	35.98		11.69		2.19		_	_	Pull out
CA-9.5$_1$	32.26	33.36	10.48	10.84	2.55	2.40	_	_	Pull out
$_2$	33.87		11.00		2.41		_	_	Pull out
$_3$	33.95		11.03		2.24		_	_	Pull out
M-$_1$	27.15	28.04	8.82	9.11	3.12	3.03	33.65	23.08	Pull out
$_2$	28.93		9.40		2.9		28.85	28.85	Pull out
$_3$	28.04		9.11		3.07		_	_	Pull out

Mix Notation	**Failure Load (kN)**	**Average Failure Load (kN)**	**Concrete Strain (‰)**		**Reinforcement Strain (‰)**				**Failure Mode**
			Right	**Left**	**1(Bottom)**	**2(Middle)**	**3(Middle)**	**4(Top)**	
CA-25$_1$	124.05	125.21	-25.51	-16.51	67.28	494.7	4384.25	9940.47	splitting
$_2$	126.04		-20.76	-26.76	33.01	644.76	_	9974.24	splitting
$_3$	125.54		_	_	_	_	_	_	splitting
CA-19$_1$	123.09	124.51	_	_	_	_	_	_	splitting
$_2$	124.9		_	_	_	_	_	_	splitting
$_3$	125.54		_	_	_	_	_	_	splitting
CA-12.5$_1$	119.98	118.37	_	_	_	_	_	_	splitting
$_2$	116.29		_	_	_	_	_	_	splitting
$_3$	118.84		_	_	_	_	_	_	splitting
CA-9.5$_1$	116.85	116.41	_	_	_	_	_	_	splitting
$_2$	114.76		_	_	_	_	_	_	splitting
$_3$	117.61		_	_	_	_	_	_	splitting
M-1$_1$	77.8	77.76	-56.19	-91.43	146.67	1305.71	_	2242.86	splitting
$_2$	79.83		-58.1	-93.33	97.14	1299.05	_	2348.57	splitting
$_3$	75.64		_	_	_	_	_	_	splitting
M-2$_1$	63.2	62.76	_	_	_	_	_	_	splitting
$_2$	64.78		_	_	_	_	_	_	splitting
$_3$	60.31		_	_	_	_	_	_	splitting
M-3$_1$	50.22	50.47	-32.52	-27.26	13.27	127.3	240.1	627.16	splitting
$_2$	49.41		-31.43	-25.71	11.43	123.81	_	624.76	splitting
$_3$	51.79		_	_	_	_	_	_	splitting

Appendix F - Laboratory Experiment Sample Pictures

Sample testing

Sieving fine aggregate

Washing fine aggregate